PHYSICAL REVIEW B **79**, 144302 (2009)

Multiscale simulation of polymer melt viscoelasticity: Expanded-ensemble Monte Carlo coupled with atomistic nonequilibrium molecular dynamics

Chunggi Baig* and Vlasis G. Mavrantzas†
Department of Chemical Engineering, University of Patras and FORTH-ICE/HT, Patras, GR 26504, Greece
(Received 22 November 2008; revised manuscript received 17 February 2009; published 14 April 2009)

We present a powerful framework for computing the viscoelastic properties of polymer melts based on an efficient coupling of two different atomistic models: the first is represented by the nonequilibrium molecular dynamics method and is considered as the microscale model. The second is represented by a Monte Carlo (MC) method in an expanded statistical ensemble and is free from any long time scale constraints. Guided by recent developments in nonequilibrium thermodynamics, the expanded ensemble incorporates appropriately defined "field" variables driving the corresponding structural variables to beyond equilibrium steady states. The expanded MC is considered as the macroscale solver for the family of all viscoelastic models built on the given structural variable(s). The explicit form of the macroscopic model is not needed; only its structure in the context of the general equation for the nonequilibrium reversible irreversible coupling or generalized bracket formalisms of nonequilibrium thermodynamics is required. We illustrate the method here for the case of unentangled linear polymer melts, for which the appropriate structural variable to consider is the conformation tensor $\tilde{\mathbf{c}}$. The corresponding Lagrange multiplier is a tensorial field $\boldsymbol{\alpha}$. We have been able to compute *model-independent* values of the tensor $\boldsymbol{\alpha}$, which for a wide range of strain rates (covering both the linear and the nonlinear viscoelastic regimes) bring results for the overall polymer conformation from the two models (microscale and macroscale) on top of each other. In a second step, by comparing the computed values of $\boldsymbol{\alpha}$ with those suggested by the macroscopic model addressed by the chosen structural variable(s), we can identify shortcomings in the building blocks of the model. How to modify the macroscopic model in order to be consistent with the results of the coupled micro-macro simulations is also discussed. From a theoretical point of view, the present multiscale modeling approach provides a solid framework for the design of improved, more accurate macroscopic models for polymer melts.

DOI: 10.1103/PhysRevB.79.144302 PACS number(s): 47.11.−j, 83.10.−y, 83.60.−a, 02.70.−c

I. INTRODUCTION

Polymers are highly complex macromolecular materials involving a multiplicity of time and length scales. For example, characteristic times involved in chain mobility span scales from 10^{-14} s (associated with bond vibrations) to seconds (characterizing chain end-to-end vector decorrelation in entangled melts) to years (connected with dynamics in the glassy state) while characteristic lengths span scales from angstroms (corresponding to bond lengths) to nanometers (corresponding to the average chain size) to micrometers (corresponding to domain size in semicrystalline structures). Understanding the complex interplay between molecular structure, conformation and architecture and macroscopic rheological response is of extreme importance in our ability to design materials with optimal properties. Equally important, however, is our ability to encode this understanding in the form of suitable constitutive equations capable of providing a reliable expression for the stress tensor in terms of the imposed flow kinematics and certain molecular parameters or material functions. For simple fluids, the Navier Stokes equations with a simple expression for the stress tensor (solely in terms of the velocity gradient tensor) provide an accurate description of their flow dynamics in almost all situations. This is not the case for complex fluids characterized by an internal microstructure: here, models derived empirically or without reference to molecular physics usually fail to represent even qualitative features of the material behavior. For polymer melts, in particular, theoretical treatments of their viscoelastic behavior based on the concept of chemical or physical cross-links (described as points or junctions at which connecting portions of molecules are forced to move together at all times) have motivated a description in terms of internal structural variables, usually a tensorial variable such as the Finger strain tensor $\mathbf{F}$ or, preferably, the conformation tensor $\tilde{\mathbf{c}}$.[1–13] Classical molecular theories of rubberlike elasticity, for example, often postulate that the Helmholtz free energy A of the underlying temporary network structure (which has been deformed by the flow) is separable into a liquidlike nonelastic (independent of deformation) and an elastic (dependent on deformation) part which depends on an appropriately defined tensorial variable $\mathbf{X}$. Based on such an idea, a number of macroscopic viscoelastic models have been developed by taking A to be of the form $\frac{A}{N_{\mathrm{ch}}} = \frac{A}{N_{\mathrm{ch}}}(\rho, T, \mathbf{X})$ where A stands for the extensive Helmholtz free energy, N_{ch} for the number of chains, ρ for the mass density, and T for the absolute temperature.[10,12]

Conformation tensor based viscoelastic models are usually closed-form differential, nonseparable constitutive equations. They represent a family of models widely used by rheologists in order to analyze complicated polymer flow problems with considerable success, since they are easy to solve numerically as they do not require tracking fluid elements. Typical examples include the upper-convected Maxwell (UCM),[8] the Giesekus,[14] the Phan-Thien/Tanner (PTT),[15,16] and the Leonov[17,18] models, as well as modifications accounting for finite extensibility with nonlinear molecular stretching,[8,19–23] nonaffine deformation,[24,25] variation

in the longest chain relaxation time with chain conformation,[26,27] and bounded free energy,[28] either separately or all together.[29] Of course, in addition to a single conformation tensor, one can envision higher-mode conformation tensor viscoelastic equations corresponding to the Rouse or bead-spring chain model. In general,[8,30] from an N-mer chain, $N(N-1)/2$ different conformation tensors $\tilde{\mathbf{c}}_{ij}$ with $i,j=1,2,\ldots,N-1$, can be constructed, each one being identified with a properly normalized average dyadic $\langle \mathbf{Q}_i \mathbf{Q}_j \rangle$, with $\mathbf{Q}_i$ denoting the connector vector between mers $i+1$ and i along the chain.

Despite all the efforts to derive accurate macroscopic models for complex fluids such as polymers, it is true that in many cases these are phenomenological or approximate; it is also true that, often, certain empirical closures should be introduced which are not always well understood or justified.[8] It is only by providing input from a more detailed microscopic model that one can avoid empiricism and approximations in the construction of the macroscopic model. Over the last years, such an approach has given rise to the development and implementation of various multiscale modeling methods. Typical examples include the use of Brownian configurational fields,[31,32] methods for the seamless, concurrent coupling of length scales,[33] heterogeneous multiscale methods (or HMM) where the word "heterogeneous" emphasizes that models of different nature can be employed at different scales [e.g., molecular dynamics (MD) at the micro scale and continuum mechanics at the macro scale],[34–36] equation-free, coarse-grained methods enabling microscopic simulators to perform system-level analysis (this is done through interpolation in space and extrapolation in time of ensemble-averaged macroscale quantities obtained from the microscopic simulations),[37] MD with absorbing boundary conditions for multiscale modeling,[38] as well as hybrid, time-scale-bridging MD methods.[39]

The present work provides the framework for designing a different class of multiscale, multiphysics methods for the study of complex materials under an applied steady flow by coupling an accurate microscopic model with a very efficient Monte Carlo (MC) method [called general equation for the nonequilibrium reversible irreversible coupling (GENERIC) MC to emphasize that it is built on the GENERIC formalism of nonequilibrium thermodynamics][12,30] in an expanded ensemble playing the role of a simulator (a solver) for the theoretical macroscopic model. The expanded ensemble includes field variables (accounting for flow effects) which drive the corresponding structural variables away from equilibrium. The idea was introduced by Mavrantzas and Theodorou[13] who employed it to simulate a polymeric system subjected to a homogeneous, steady-state extensional flow at constant elongation rate in one direction (this has perhaps the simplest kinematical structure in nonequilibrium MC simulations of flowing systems); they did so by considering the conjugate thermodynamic variable to $\tilde{\mathbf{c}}$, the tensorial orienting field $\boldsymbol{\alpha}$, intimately related to the strain rate in the flow situation. Although no systematic connection was made between the synthetic field $\boldsymbol{\alpha}$ used in the MC simulations and the rate-of-strain tensor $\dot{\boldsymbol{\gamma}}$ employed in the actual flow, that attempt demonstrated how one can drive a system away from equilibrium by using synthetic fields in the context of a nondynamic method. In a later work,[30] the methodology was rigorously formulated in the context of the GENERIC formalism of nonequilibrium thermodynamics; it was consequently termed GENERIC MC. The formal generalization served as the starting point for designing a rigorous (Hamiltonian-based) statistical mechanics framework for unknown nonequilibrium systems through field variables defined as the conjugate variables (the Lagrange multipliers) of appropriately introduced structural variables describing the system in an overall sense. In a flow situation, these structural parameters (slow dynamical variables) depart from their values in the quiescent fluid, while all other (faster) degrees of freedom track the evolution of the structural parameters; i.e., they are assumed to be at equilibrium subject to the constraints imposed by the values of the structural parameters at all times.[13] The key (perhaps the most important) step in the method is the choice of the proper set of the state variables, $\mathbf{x}$, effectively representing nonequilibrium states.[12,40]

Quite recently, it was demonstrated[41] that GENERIC MC can generate realistic nonequilibrium structures under an external flow field similar to those obtained through the direct application of a true dynamic method. From a mathematical point of view, this is equivalent to establishing a relationship between the synthetic thermodynamic force fields introduced in the extended statistical ensemble and the true velocity field assumed in the actual flow. The connection was achieved by determining the synthetic field iteratively so that, for a given value of the shear rate, the resulting value of the corresponding structural variable is equal to that calculated through independent nonequilibrium molecular dynamics (NEMD) simulations. Preliminary (test) simulations with a $C_{50}H_{102}$ polyethylene liquid showed the two methods (expanded MC and NEMD) to provide identical results for $\tilde{\mathbf{c}}$.[41]

The purpose of this work is to present the GENERIC MC method in detail, to analyze its statistical mechanics foundations, and to demonstrate how it can serve as a useful framework for multiscale modeling, linking conventional and widely used macroscopic models with microscopic complex systems behavior. We will see that it is possible to sample statistically appropriate nonequilibrium phase-space points corresponding to an imposed external field guided by a coarser, macroscopic-level model, without adhering to its specific mathematical expression. All that is needed is the choice of variables and the corresponding GENERIC structure of the fundamental evolution equation. As noted by Öttinger:[40] "Beyond equilibrium, and contrary to our equilibrium experience, this choice is far from obvious. Actually, this is the point at which the most physical intuition is required. A poor choice of $\boldsymbol{x}$ cannot be repaired by even the most ingenious formulation of thermodynamic building blocks. For example, for the famous reptation (reptile-like or snake-like) model of a melt of entangled linear polymer molecules, considered later, the idea of smooth primitive paths, and the corresponding configurational distribution function, are the keys to success."

The most important features of the proposed framework are the following: (a) it allows modeling the macroscale quantities of interest by coupling with a microscale model without using the explicit form of the macroscopic model.

(b) The microscopic model is a remarkably accurate (atomistic) model. A number of studies in the last few years[42,43] have shown it to provide excellent predictions of the structural, conformation, and volumetric properties of several polymers (polyethylene, polybutadiene, polyisobutelene, H-shaped polyethylene, etc.) over a wide range of temperature and pressure conditions. (c) The macroscopic solver is based on a powerful set of chain connectivity altering moves allowing the robust sampling of configurational space.[44] (d) The choice of the structural variables in the expanded MC solver and of their corresponding Lagrange multipliers is guided from nonequilibrium thermodynamics; as such they bear a direct connection with available macroscopic viscoelastic models widely employed in numerical and theoretical studies of polymer melt viscoelasticity. (e) Combined with the results of some additional, direct dynamic simulations and the use of the Green-Kubo formulae,[12,40,45,46] one can fully compute the underling friction or relaxation matrix of the macroscopic model. (f) Structural variables of totally different nature can be addressed (tensors or distribution functions).[47–50] (g) The macroscale model is a high fidelity solver providing feedback to the analytical viscoelastic model for the chosen structural variable. This can be used to parametrize the macroscopic model but also to correct the functional form of its building blocks (we provide an example here). This is in line with the comment of Brandt[51] that one might be able to construct an effective macroscopic model from data accumulated during the computation with a multiscale model.

The main disadvantages of the approach are the following: (a) the underlying atomistic MC algorithm is available today only for a limited number of polymers (such as polyethylene, polypropylene, and polybutadiene). Efforts are, however, in progress to generalize it for more complicated structures and architectures through coarse-grained strategies that preserve chain stereochemistry.[52] (b) Being nondynamic in nature, the macroscopic solver (GENERIC MC) can address only the steady-state properties of the fluid at conditions beyond equilibrium. It provides no information about the transient behavior. (c) The microscopic solver (NEMD) is available today only for shear and planar elongational flows. This implies that it cannot handle arbitrary flows; for example, how to modify the boundary conditions to treat one-dimensional or uniaxial extensional flows is not yet known.

The paper is organized as follows. In Sec. II, we present the basic ingredients of the GENERIC formalism and all details of the proposed framework (these refer to both the direct microscopic model, i.e., the NEMD method and the GENERIC MC simulator of the macroscopic model), with a focus on systems described at the coarse-grained or macroscopic level by a tensorial structural variable (here $\tilde{\mathbf{c}}$). In Sec. III, we discuss the types of polymeric systems simulated here and the results obtained. We provide the relationship between the synthetic field used in the GENERIC MC simulations and the actual shear rate employed in the microscopic simulations for a number of PE melts, we present the results obtained for the conformation tensor from the two solvers and how they compare with each other, and we comment on their differences and how these are related to the choice of the synthetic field or to the functional form of the friction matrix of the macroscopic model. To illustrate the capabilities of the macrosolver, some additional results are presented in Sec. III referring to structure descriptors at shorter length scales. We will see that GENERIC MC provides an excellent description of the simulated systems even at scales shorter than the chain end-to-end vector (that was designed for). This is a unique, very encouraging result because it justifies the choice of the conformation tensor as the appropriate primary variable at the coarse-grained level: at a given value of the conformation tensor $\tilde{\mathbf{c}}$ (or its conjugate field $\boldsymbol{\alpha}$), all possible configurations that the microscopic system can adopt at the given temperature and density conditions are indeed categorized according to that value of $\tilde{\mathbf{c}}$ (or $\boldsymbol{\alpha}$).[13] Concluding remarks are made in Sec. IV.

II. SIMULATION METHODOLOGY

Our multiscale modeling approach aims at offering a satisfactory description of the viscoelastic behavior of a polymeric fluid through a hierarchical approach wherein different models are employed to describe the system at different length and time scales. For the approach to be successful, the flow of information from one level to the other should be based on a well-founded (if possible, molecular) theory providing the link in terms of a mathematical framework. This can help overcome computational challenges associated with high-resolution calculations at the interface of two levels. For the case considered here, consistency during level bridging is achieved by considering simultaneously two solvers of totally different nature for the system: the first is the NEMD method for an atomistic system. The second is MC in an expanded statistical ensemble. The bridging of the two methods is achieved by computing the extra synthetic fields entering the latter guided by a macroscopic theory, the GENERIC approach to nonequilibrium thermodynamics. GENERIC provides the vector of pertinent state variables at the macroscopic level and an expression for the general form of the underlying friction or relaxation matrix that satisfies the two fundamental laws: the second law of thermodynamics and the Onsager-Casimir reciprocity relationships of linear irreversible thermodynamics.

The structural variables should not be chosen arbitrarily: they should bear connection with available macroscopic viscoelastic models employed quite widely in numerical and theoretical studies of polymer melt viscoelasticity. Once the state variables have been identified, one can define their corresponding thermodynamic fields: these form a set of Lagrange multipliers intimately related to the velocity gradient in a homogeneous steady flow. It is these fields that are introduced in the expanded MC method to enable the simulation of the system under beyond-equilibrium conditions. We will say that the two models have been consistently coupled if their results for a given flow field are identical, implying that the values of the synthetic fields entering the expanded-ensemble MC simulations have been chosen correctly. The computation of the synthetic fields will be the most important result of such a methodology, since these are in essence the elements of the friction or relaxation matrix of

the macroscopic GENERIC model onto which the expanded-ensemble MC methodology was founded.[30] Given a thermodynamically admissible thermodynamic model, therefore, the success of the proposed approach lies in the construction of a combined, "added-value" micro-macro solver which (a) borrows from the macroscopic model just its main building blocks (but not their exact mathematical expression) and (b) returns information allowing the complete parametrization of the model based on atomistic-level data.

A. Fundamental aspects of the GENERIC formalism of nonequilibrium thermodynamics

If $\mathbf{x}$ is the vector of state variables describing a dynamical system beyond equilibrium (this typically contains position-dependent fields such as the local mass, momentum and energy densities of hydrodynamics, and one or more structural variables), then its fundamental evolution equation in the GENERIC formalism reads[12]

$$\frac{\partial \mathbf{x}}{\partial t} = \mathbf{L}(\mathbf{x}) \cdot \frac{\delta E(\mathbf{x})}{\delta \mathbf{x}} + \mathbf{M}(\mathbf{x}) \cdot \frac{\delta S(\mathbf{x})}{\delta \mathbf{x}}, \tag{1}$$

where E and S represent the total energy and entropy of the system, $\mathbf{L}$ is a Poisson matrix that turns energy gradients into reversible dynamics, and $\mathbf{M}$ a friction matrix that turns entropy gradients into irreversible dynamics. $\mathbf{L}$ is always antisymmetric while $\mathbf{M}$ is usually symmetric expressing the famous Onsager-Casimir symmetry of linear irreversible thermodynamics.[12,40,53] The two generators E and S of reversible and irreversible thermodynamics and the matrices $\mathbf{L}$ and $\mathbf{M}$ are further restricted to satisfy the following two mutual degeneracy conditions:

$$\mathbf{L}(\mathbf{x}) \cdot \frac{\delta S(\mathbf{x})}{\delta \mathbf{x}} = 0, \quad \mathbf{M}(\mathbf{x}) \cdot \frac{\delta E(\mathbf{x})}{\delta \mathbf{x}} = 0, \tag{2}$$

representing physically the decoupling nature of reversibility and irreversibility. The vector $\mathbf{x}$ of the set of (thermodynamic) state variables is typically expressed as $\mathbf{x} = \{\rho(\mathbf{r}), \mathbf{M}(\mathbf{r}), \varepsilon(\mathbf{r}), \mathbf{X}(\mathbf{r})\}$, where the mass density ρ, the momentum density $\mathbf{M}$, the internal energy ε, and the structural variable $\mathbf{X}$ characterizing nonequilibrium states are generally functions of the position vector $\mathbf{r}$. Assuming that most of the external-field effects on the overall structure of the system are absorbed into the entropy functional (i.e., the energetic effect is relatively negligible), E and S are commonly expressed as

$$E(\mathbf{x}) = \int \left[\frac{\mathbf{M}(\mathbf{r})^2}{2\rho(\mathbf{r})} + \varepsilon(\mathbf{r}) \right] d\mathbf{r}, \tag{3a}$$

and

$$S(\mathbf{x}) = \int s[\rho(\mathbf{r}), \varepsilon(\mathbf{r}), \mathbf{X}(\mathbf{r})] d\mathbf{r}. \tag{3b}$$

The proper choice of $\mathbf{X}$ is clearly crucial in determining nonequilibrium thermodynamic functions. The general thermodynamic equation for the entropy density s in GENERIC is written as[12,30]

$$s(\mathbf{x}) = k_B \sum_k \lambda_k x_k, \tag{4a}$$

or, equivalently, as

$$ds = k_B \sum_k \lambda_k dx_k, \tag{4b}$$

from which the Lagrange multipliers λ_k are naturally defined as

$$\frac{\delta S(\mathbf{x})}{\delta x_k} = k_B \lambda_k, \tag{5}$$

where k_B is Boltzmann's constant. Furthermore, by taking the total derivative of Eq. (4a) and by comparing with Eq. (4b), one derives the generalized Gibbs-Duhem relation

$$\sum_k x_k d\lambda_k = 0. \tag{6}$$

Using Eqs. (4a), (4b), (5), and (6), the fundamental thermodynamic equations for the rest of the free-energy functions of the nonequilibrium system can be derived in a straightforward manner, using appropriate Legendre transforms.

Based on the fundamental statistical principle of *the equal a priori probability for every phase-space point at a constant energy surface*,[54] the probability density function $\rho_{[\lambda]}$ in the generalized canonical GENERIC statistical ensemble corresponding to the above macroscopic thermodynamic relations is[12]

$$\rho_{[\boldsymbol{\lambda}]}(\mathbf{z}) = \frac{1}{Q(\boldsymbol{\lambda})} \exp\left(- \sum_k \lambda_k \Pi_k(\mathbf{z}) \right), \tag{7}$$

$$Q(\boldsymbol{\lambda}) = \int \exp\left(- \sum_k \lambda_k \Pi_k(\mathbf{z}) \right) d\mathbf{z},$$

where $\mathbf{z}$ represents the full phase space comprising both the position ($\mathbf{r}$) and momentum ($\mathbf{p}$) coordinates of all particles in the system. The extensive thermodynamic variable Π_k [whose ensemble average corresponds to the thermodynamic state variable, $x_k = \langle \Pi_k(\mathbf{z}) \rangle_{[\boldsymbol{\lambda}]} = \int \rho_{[\boldsymbol{\lambda}]}(\mathbf{z}) \Pi_k(\mathbf{z}) d\mathbf{z}$] is paired with its conjugate thermodynamic field, the Lagrange multiplier λ_k. The Boltzmann factors of all pairs are combined (i.e., multiplied) to generate appropriate phase space that sample system configurations under the conditions imposed externally by the λ_k's. Thus, the most fundamental statistical expression for the entropy functional is written as[55]

$$S(\mathbf{x}) = -k_B \int \rho_{[\boldsymbol{\lambda}]}(\mathbf{z}) \ln[\rho_{[\boldsymbol{\lambda}]}(\mathbf{z})] d\mathbf{z} = k_B \left[\ln Q(\boldsymbol{\lambda}) + \sum_k \lambda_k x_k \right]. \tag{8}$$

Using Eqs. (1) and (5), one can show that the Lagrange multipliers obey the following kinematic equation under steady-state conditions:

$$\boldsymbol{\lambda} = -\frac{1}{k_B} \mathbf{M}^{-1} \cdot \mathbf{L}(\mathbf{x}) \cdot \frac{\delta E(\mathbf{x})}{\delta \mathbf{x}}. \tag{9}$$

TABLE I. The functional form of the $f_1(I_1)$, $f_2(I_1)$, $f_3(I_1)$, and $f_4(I_1)$ functions, in the general expression of the relaxation matrix $\mathbf{\Lambda}$ [Eq. (14)], for several viscoelastic models.

Model	$f_1(I_1)$	$f_2(I_1)$	$f_3(I_1)$	$f_4(I_1)$
UCM, FENE	$\frac{1}{2\lambda_0 n k_B T}$	0	0	0
Giesekus	$\frac{1}{2\lambda_0 n k_B T}(1-\alpha)$	$\frac{1}{2\lambda_0 n k_B T}\alpha$	0	0
PTT	$\frac{1}{2\lambda_0 n k_B T}\exp[(1-\xi)\varepsilon(I_1-3)]$	0	0	0
Extended White/Metzner	$\frac{1}{2\lambda_0 n k_B T}\left(\frac{I_1}{3}\right)^{-k}$	0	0	0
Modified Bird-DeAguiar	$\frac{1}{2\lambda_0 n k_B T}\sigma$	0	0	$\frac{2}{\lambda_0 n k_B T}\frac{1-\sigma}{I_1}$
Leonov	0	$\frac{1}{2\lambda_0 n k_B T}$	0	$-\frac{2}{3\lambda_0 n k_B T}$
Hybrid FENE/PTT/Giesekus[a]	$\frac{1}{2\lambda_0 n k_B T}[1-\alpha(1-\xi)]$ $\times\exp\{(1-\xi)\varepsilon[I_1 h_0(I_1)-3]\}$	$\frac{1}{2\lambda_0 n k_B T}\alpha(1-\xi)h_0(I_1)$ $\times\exp\{(1-\xi)\varepsilon[I_1 h_0(I_1)-3]\}$	0	0

[a]In this model, the exact form of the spring constant $h_0(I_1)$ depends on the specific model; for example, $h_0(I_1)=\frac{b-3}{b-I_1}$ for the FENE-Peterlin approximation and $h_0(I_1)=\frac{3(b-2)b-I_1}{3(b-I_1)}$ for the FENE-Cohen approximation. More details can be found in Ref. 29.

B. GENERIC formalism for polymer melts coarse grained to the level of conformation tensor

Descriptions of polymeric systems in terms of internal structural parameters quantify chain conformation in an overall sense. In the literature, the conformation tensor $\tilde{\mathbf{c}}$ is defined mathematically as[8,13]

$$\tilde{c}_{\alpha\beta}=\frac{3\langle R_\alpha R_\beta\rangle}{\langle R^2\rangle_{\mathrm{eq}}}, \tag{10}$$

where $\mathbf{R}$ denotes the chain end-to-end vector and the subscript eq equilibrium conditions. According to Eq. (10), at equilibrium (no flow) and away from any boundaries, $\tilde{\mathbf{c}}$ is equal to the unit tensor $\boldsymbol{\delta}$.

With the choice $\mathbf{X}=\tilde{\mathbf{c}}$, according to the GENERIC (Ref. 12) or generalized bracket formalisms[10] of nonequilibrium thermodynamics, the constitutive equation for the viscoelastic material takes the following general form:

$$\frac{\partial\tilde{c}_{\alpha\beta}}{\partial t}+v_\gamma\nabla_\gamma\tilde{c}_{\alpha\beta}-(\nabla_\gamma v_\alpha)\tilde{c}_{\gamma\beta}-\tilde{c}_{\alpha\gamma}\nabla_\gamma v_\beta=-\Lambda_{\alpha\beta\gamma\varepsilon}\frac{\delta A(\tilde{\mathbf{c}})}{\delta\tilde{c}_{\gamma\varepsilon}}, \tag{11}$$

while the (elastic) stress tensor is defined according to

$$\tau_{\alpha\beta}=2c_{\alpha\gamma}\frac{\delta A(\tilde{\mathbf{c}})}{\delta\tilde{c}_{\gamma\beta}}. \tag{12}$$

On the left-hand side of Eq. (11) we recognize the upper-convected Maxwell derivative of $\tilde{c}_{\alpha\beta}$:

$$\hat{\tilde{c}}_{\alpha\beta}\equiv\frac{\partial\tilde{c}_{\alpha\beta}}{\partial t}+v_\gamma\nabla_\gamma\tilde{c}_{\alpha\beta}-(\nabla_\gamma v_\alpha)\tilde{c}_{\gamma\beta}-\tilde{c}_{\alpha\gamma}\nabla_\gamma v_\beta, \tag{13}$$

and on the right-hand side the appearance of the fourth-rank relaxation matrix $\mathbf{\Lambda}$ and the free-energy functional A. Note also the use of the Einstein summation convention over repeated indices, e.g., $a_\gamma b_\gamma=\Sigma_\gamma a_\gamma b_\gamma$. The relaxation matrix $\mathbf{\Lambda}$ has to satisfy Onsager's symmetry property and the thermodynamic admissibility criteria (i.e., the second law of thermodynamics). The free energy A, on the other hand, is usually taken to be a function of the invariants of the conformation tensor $\tilde{\mathbf{c}}$. With suitable choices of $\mathbf{\Lambda}$ and A, a number of well-established and widely used viscoelastic models are reproduced. These include the UCM, the Giesekus, the PTT, the finitely extensible nonlinear elastic (FENE), the hybrid FENE/PTT/Giesekus, the modified Bird-DeAguiar, and the extended White-Metzner models. From the point of view of the GENERIC formalism of nonequilibrium thermodynamics, all these expressions for $\mathbf{\Lambda}$ are particular cases of the following more general construction:[10]

$$\begin{aligned}\Lambda_{\alpha\beta\gamma\varepsilon}(\tilde{\mathbf{c}})=&f_1(I_1)(\tilde{c}_{\alpha\gamma}\delta_{\beta\varepsilon}+\tilde{c}_{\alpha\varepsilon}\delta_{\beta\gamma}+\tilde{c}_{\beta\gamma}\delta_{\alpha\varepsilon}+\tilde{c}_{\beta\varepsilon}\delta_{\alpha\gamma})\\&+2f_2(I_1)(\tilde{c}_{\alpha\gamma}\tilde{c}_{\beta\varepsilon}+\tilde{c}_{\alpha\varepsilon}\tilde{c}_{\beta\gamma})\\&+f_3(I_1)(\tilde{c}_{\alpha\beta}\delta_{\gamma\varepsilon}+\tilde{c}_{\gamma\varepsilon}\delta_{\alpha\beta})+f_4(I_1)(\tilde{c}_{\alpha\beta}\tilde{c}_{\gamma\varepsilon}),\end{aligned} \tag{14}$$

where I_1 is the first invariant of $\tilde{\mathbf{c}}$ (the trace of $\tilde{\mathbf{c}}$), $\boldsymbol{\delta}$ is the second-rank unit tensor, and f_1, f_2, f_3, and f_4 are arbitrary functions of I_1. A, on the other hand, is usually assumed to be a function of all three invariants of $\tilde{\mathbf{c}}$. Table I summarizes the choices of $\mathbf{\Lambda}$ that reproduce the above-mentioned viscoelastic models. We further note that in order for the model to

satisfy the second law of thermodynamics (the rate of entropy production should be non-negative), namely, $\frac{\delta A}{\delta \tilde{\mathbf{c}}_{\alpha\beta}}\Lambda_{\alpha\beta\gamma\varepsilon}\frac{\delta A}{\delta \tilde{\mathbf{c}}_{\gamma\varepsilon}} \geq 0$, $f_1(I_1)$, $f_2(I_1)$, $f_3(I_1)$, and $f_4(I_1)$ must be constrained to certain limits.[10,29] Certain special cases are considered in Appendix A leading to

$$f_i(I_1) \geq 0, \quad \forall\, i. \tag{15}$$

C. Coupled NEMD-GENERIC MC multiscale modeling methodology

Separating temperature effects (based on the well-known notion of purely entropic spring force from the theory of network models) from the Lagrange multiplier,[8] the general expression for the internal energy function of polymeric systems under flow is written as

$$U = TS - PV + \mu N_{\mathrm{ch}} + N_{\mathrm{ch}} k_B T \boldsymbol{\alpha}:\tilde{\mathbf{c}}, \tag{16a}$$

implying that

$$dU = TdS - PdV + \mu dN_{\mathrm{ch}} + k_B T \boldsymbol{\alpha}:d(N_{\mathrm{ch}}\tilde{\mathbf{c}}). \tag{16b}$$

From these equations, all other thermodynamic functions can be derived through appropriate Legendre transforms.[56] For example, the extended Helmholtz free energy A and Gibbs free energy G of the nonequilibrium system will be given through

$$dA(T,V,N_{\mathrm{ch}},N_{\mathrm{ch}}\tilde{\mathbf{c}}) = -SdT - PdV + \mu dN_{\mathrm{ch}} + k_B T \boldsymbol{\alpha}:d(N_{\mathrm{ch}}\tilde{\mathbf{c}}), \tag{17a}$$

and

$$dG(T,P,N_{\mathrm{ch}},\boldsymbol{\alpha}) = -SdT + VdP + \mu dN_{\mathrm{ch}} - N_{\mathrm{ch}} k_B T \tilde{\mathbf{c}}:d\boldsymbol{\alpha}, \tag{17b}$$

respectively. Equation (17b) is the one employed in the original Mavrantzas-Theodorou work.[13] The Helmholtz free-energy density can alternatively be written as

$$d\left(\frac{A}{V}\right) = -\frac{S}{V}dT + \mu d\left(\frac{N_{\mathrm{ch}}}{V}\right) + k_B T \boldsymbol{\alpha}:d\left(\frac{N_{\mathrm{ch}}}{V}\tilde{\mathbf{c}}\right). \tag{18}$$

According to Eqs. (5) and (18), it is thus recognized that

$$\boldsymbol{\lambda}_{\tilde{\mathbf{c}}} = \frac{1}{k_B}\frac{\delta S}{\delta \tilde{\mathbf{c}}} = -\frac{1}{k_B T}\frac{\delta A(\tilde{\mathbf{c}})}{\delta \tilde{\mathbf{c}}} = -\frac{N_{\mathrm{ch}}}{V}\boldsymbol{\alpha}. \tag{19}$$

Based on the above generalized thermodynamic equations, we are now ready to design a consistent micro-macro simulation method capable of addressing flow effects on the conformation of unentangled polymer melts. For simplicity, we restrict ourselves to the case of steady shear described by the following velocity gradient tensor:

$$\nabla\mathbf{u} = \begin{pmatrix} 0 & 0 & 0 \\ \dot{\gamma} & 0 & 0 \\ 0 & 0 & 0 \end{pmatrix}. \tag{20}$$

1. Micromodel

The micromodel is a high-resolution model addressing phenomena at the atomistic level. In the present work, it is represented by the NEMD method.[57–61] The method extends the classical MD technique for equilibrium systems to account for flow effects. Following Baig *et al.*,[61] in particular, the method is described by the following set of evolution equations:

$$\dot{\mathbf{q}}_i = \frac{\mathbf{p}_i}{m_i} + \mathbf{q}_i \cdot \nabla\mathbf{u},$$

$$\dot{\mathbf{p}}_i = \mathbf{F}_i - \mathbf{p}_i \cdot \nabla\mathbf{u} - m_i \mathbf{q}_i \cdot \nabla\mathbf{u} \cdot \nabla\mathbf{u}, \tag{21a}$$

where $\nabla\mathbf{u}$ denotes the imposed velocity gradient, m_i the mass of atom i, and $(\mathbf{q}_i, \mathbf{p}_i)$ are the generalized coordinates (position and momentum) of atom i in the system. These equations satisfy Newton's law, i.e., $m_i\ddot{\mathbf{q}}_i = \mathbf{F}_i$ where $\mathbf{F}_i(=-\frac{\partial U}{\partial \mathbf{q}_i})$ denotes the force on atom i due to intra- and intermolecular interactions with all other atoms in the system and $U = U(\mathbf{q}_i)$ the corresponding potential energy function. The set (21a) is known as the p-SLLOD equations of motion, and with a Nosé-Hoover thermostat,[62,63] it takes the form

$$\dot{\mathbf{q}}_i = \frac{\mathbf{p}_i}{m_i} + \mathbf{q}_i \cdot \nabla\mathbf{u},$$

$$\dot{\mathbf{p}}_i = \mathbf{F}_i - \mathbf{p}_i \cdot \nabla\mathbf{u} - m_i \mathbf{q}_i \cdot \nabla\mathbf{u} \cdot \nabla\mathbf{u} - \frac{p_\eta}{Q}\mathbf{p}_i,$$

$$\dot{\eta} = \frac{p_\eta}{Q},$$

$$\dot{p}_\eta = \sum_i \frac{\mathbf{p}_i^2}{m_i} - dk_B T, \tag{21b}$$

where η is the additional degree of freedom (the thermostat) playing the role of a heat bath whose aim is to damp out temperature deviations from the desired level, Q its effective mass, p_η its momentum, and d the total degrees of freedom of the system. Together with the Lees-Edwards boundary conditions for the case of shear[64] or the Kraynik-Reinelt ones for the case of planar extension,[65] the set of equations in Eq. (21b) allows simulating a polymer melt at constant temperature under the application of an external flow field and defines the micromodel here.

2. Macromodel

The macromodel is represented in this work by the GENERIC MC method.[30] Following Mavantzas-Theodorou[13] and Mavrantzas-Öttinger,[30] this is realized in an expanded semigrand statistical ensemble $\{N_{\mathrm{ch}}NPT\boldsymbol{\mu}^*\boldsymbol{\alpha}\}$, in which the following variables are specified (held fixed): the number of chains N_{ch}, the average number of atoms per chain N, the pressure P, the temperature T, the spectrum of chain relative chemical potentials $\boldsymbol{\mu}^*$ controlling the distribution of chain lengths in the system (and thus also the system polydispersity)[66] and the tensorial field $\boldsymbol{\alpha}$ accounting for flow effects. As explained in the previous section, the field $\boldsymbol{\alpha}$ couples with the conformation tensor $\tilde{\mathbf{c}}$ and drives polymer configurations away from their spherical shape representative

of a quiescent (no flow applied) equilibrium system. The corresponding probability density function is

$$\rho^{N_{\mathrm{ch}}NPT\boldsymbol{\mu}^*\boldsymbol{\alpha}}(\mathbf{r}_1,\mathbf{r}_2,\ldots,\mathbf{r}_n,V) \sim \exp\left\{-\beta\left[U(\mathbf{r}_1,\mathbf{r}_2,\ldots,\mathbf{r}_n,V)+PV-\sum_{k=1}^{N_{\mathrm{ch}}}\mu_k^* N_k - k_B T\boldsymbol{\alpha}:\sum_{k=1}^{N_{\mathrm{ch}}}\tilde{\mathbf{c}}_k\right]\right\}, \tag{22a}$$

implying that system configurations are sampled according to the following modified Metropolis criterion:

$$p_{acc}^{N_{\mathrm{ch}}NPT\boldsymbol{\mu}^*\boldsymbol{\alpha}} \sim \exp\left\{-\beta\left[\Delta U + P\Delta V - \sum_{k=1}^{N_{\mathrm{ch}}}\Delta(\mu_k^* N_k) - k_B T\boldsymbol{\alpha}:\sum_{k=1}^{N_{\mathrm{ch}}}\Delta\tilde{\mathbf{c}}_k\right]\right\}, \tag{22b}$$

or, for the case of a system simulated under conditions of constant volume V (i.e., constant density ρ), according to

$$p_{acc}^{N_{\mathrm{ch}}NVT\boldsymbol{\mu}^*\boldsymbol{\alpha}} \sim \exp\left\{-\beta\left[\Delta U - \sum_{k=1}^{N_{\mathrm{ch}}}\Delta(\mu_k^* N_k) - k_B T\boldsymbol{\alpha}:\sum_{k=1}^{N_{\mathrm{ch}}}\Delta\tilde{\mathbf{c}}_k\right]\right\}, \tag{22c}$$

where $\beta \equiv \frac{1}{k_B T}$. In the above equations, $n(=N_{\mathrm{ch}}\times N)$ is the total number of atoms in the system, $\{\mathbf{r}\}=\{\mathbf{r}_1,\mathbf{r}_2,\ldots,\mathbf{r}_n\}$ denotes the space of their position vectors, V the volume, U the potential energy of the system, $\{\mu_k^*\}_{k=1}^{N_{\mathrm{ch}}}$ the relative chemical potential of the kth chain in the system and $\{\tilde{\mathbf{c}}_k\}_{k=1}^{N_{\mathrm{ch}}}$ its conformation tensor. With appropriate input data for the set $\{N_{\mathrm{ch}}NPT\boldsymbol{\mu}^*\boldsymbol{\alpha}\}$, such a method allows sampling phase points of the simulated polymer beyond equilibrium, by assigning nonzero values to $\boldsymbol{\alpha}$.

Precisely defining $\boldsymbol{\alpha}$ so that the kinematics of a true shear flow is generated, described by Eq. (20) above, is not a trivial task and this is where the two solvers are bridged. In general, and guided by the availability of a large number of viscoelastic models (some of which are reported in Table I), one has a number of choices. For the case of simple shear considered here, according (for example) to the simple UCM model, $\boldsymbol{\alpha}$ comes out to be

$$\boldsymbol{\alpha} = \begin{bmatrix} \frac{1}{2}\frac{(\lambda_0\dot{\gamma})^2}{1+(\lambda_0\dot{\gamma})^2} & \frac{1}{2}\frac{\lambda_0\dot{\gamma}}{1+(\lambda_0\dot{\gamma})^2} & 0 \\ \frac{1}{2}\frac{\lambda_0\dot{\gamma}}{1+(\lambda_0\dot{\gamma})^2} & -\frac{1}{2}\frac{(\lambda_0\dot{\gamma})^2}{1+(\lambda_0\dot{\gamma})^2} & 0 \\ 0 & 0 & 0 \end{bmatrix}, \tag{23}$$

where λ_0 is the longest relaxation time of the polymer. On the other hand, according to the more refined and widely used Giesekus model, the elements of $\boldsymbol{\alpha}$ (again for the case of steady shear) are obtained from the solution to the following set of algebraic equations:

$$(1-2a)\tilde{c}_{yy} + a(\tilde{c}_{xy}^2 + \tilde{c}_{yy}^2) - 1 + a = 0,$$

$$(1-2a)\tilde{c}_{xy} + a(\tilde{c}_{xx}\tilde{c}_{xy} + \tilde{c}_{xy}\tilde{c}_{yy}) - (\lambda_0\dot{\gamma})\tilde{c}_{yy} = 0,$$

$$(1-2a)\tilde{c}_{xx} + a(\tilde{c}_{xx}^2 + \tilde{c}_{xy}^2) - 2(\lambda_0\dot{\gamma})\tilde{c}_{xy} - 1 + a = 0,$$

$$\tilde{c}_{zz} = 1, \tag{24a}$$

together with

$$\boldsymbol{\alpha} = \frac{1}{2}\lambda_0[\boldsymbol{\delta} + a(\tilde{\mathbf{c}} - \boldsymbol{\delta})]^{-1}\cdot[\boldsymbol{\nabla}\mathbf{u} + \tilde{\mathbf{c}}^{-1}\cdot\boldsymbol{\nabla}\mathbf{u}^T\cdot\tilde{\mathbf{c}}], \tag{24b}$$

where a denotes the Giesekus parameter (it usually takes values between 0 and 1/2) while $\tilde{c}_{xx}$, $\tilde{c}_{xy}=\tilde{c}_{yx}$, $\tilde{c}_{yy}$, and $\tilde{c}_{zz}$ are the values of the conformation tensor for the given polymer melt. $\tilde{\mathbf{c}}^{-1}$ is the inverse of $\tilde{\mathbf{c}}$ and $\boldsymbol{\nabla}\mathbf{u}^T$ the transpose of $\boldsymbol{\nabla}\mathbf{u}$. Similar expressions are found for the other models reported in Table I or in the literature. In any of these cases, however, the results of the macromodel will be model dependent, and thus approximate. To avoid this, we propose here a truly consistent implementation of the macromodel by determining $\boldsymbol{\alpha}$ solely from the most general expression for the underlying transport matrix $\boldsymbol{\Lambda}$ reported in Eq. (14). Accordingly, for the case of shear discussed here, $\tilde{\mathbf{c}}$ and $\boldsymbol{\alpha}$ should have only four independent and nonzero components, the sets $\{\tilde{c}_{xx},\tilde{c}_{xy}=\tilde{c}_{yx},\tilde{c}_{yy},\tilde{c}_{zz}\}$ and $\{\alpha_{xx},\alpha_{xy}=\alpha_{yx},\alpha_{yy},\alpha_{zz}\}$, respectively, implying that the most general form of the tensor $\boldsymbol{\alpha}$ which should be used in the GENERIC MC solver in order to generate a true shear flow is

$$\boldsymbol{\alpha} = \begin{pmatrix} \alpha_{xx} & \alpha_{xy} & 0 \\ \alpha_{xy} & \alpha_{yy} & 0 \\ 0 & 0 & \alpha_{zz} \end{pmatrix}, \tag{25}$$

leaving the exact dependence of the four nonzero elements α_{xx}, α_{xy}, α_{yy}, and α_{zz} on the imposed shear rate $\dot{\gamma}$ undetermined. This implies that a state point in the microscopic model, which will correspond to a given value of $\dot{\gamma}$, is represented in the macroscopic model by the set $\{\alpha_{xx},\alpha_{xy}=\alpha_{yx},\alpha_{yy},\alpha_{zz}\}$. In fact, for the majority of the members of the family of viscoelastic models reported in Table I, the coefficients f_3 and f_4 are usually taken to be zero. Then, it can be shown (see Appendix A) that $\alpha_{zz}=0$. This important simplification is also adopted in this study in order to judge its effects and test its validity; as a result, the number of the unknown components of the tensor $\boldsymbol{\alpha}$ that should be determined for a given value of shear rate $\dot{\gamma}$ reduces to three, implying that all GENERIC MC simulations performed in this work correspond to

$$\boldsymbol{\alpha} = \begin{pmatrix} \alpha_{xx} & \alpha_{xy} & 0 \\ \alpha_{xy} & \alpha_{yy} & 0 \\ 0 & 0 & 0 \end{pmatrix}. \tag{26}$$

Our proposed simulation strategy for a consistently coupled micro-macro modeling scheme includes then the following steps:

Step (1): For a given shear rate $\dot{\gamma}$ or Deborah number defined as $\mathrm{De}=\lambda_0\dot{\gamma}$, i.e., as the product of the longest relax-

ation time λ_0 of the polymer under study times the imposed shear rate $\dot{\gamma}$, carry out first the direct NEMD simulation (run the micromodel) and compute the elements of the conformation tensor $\tilde{\mathbf{c}}$. This will be the exact result for the given polymer melt subjected to the given shear rate.

Step (2): For the same given shear rate $\dot{\gamma}$, choose a set of initial values for the nonzero elements of the Lagrange multiplier $\boldsymbol{\alpha}$ (these can correspond, e.g., to the Giesekus model) and execute the GENERIC MC simulation in the expanded statistical ensemble of Eq. (22c) (macromodel) and compute the conformation tensor $\tilde{\mathbf{c}}$. Given that the macroscopic model used to estimate $\boldsymbol{\alpha}$ is not accurate, the values of $\tilde{\mathbf{c}}$ obtained from the macrosolver will be different from the exact ones computed by the microsolver.

Step (3): Use the results of steps (1) and (2) to define an improved set of values for the nonzero components of $\boldsymbol{\alpha}$ and iterate until convergence, i.e., until the value of the objective function defined as

$$F_{\text{obj}} = \sqrt{\frac{\sum_{i=1}^{n_{\text{type}}} w_i[(R_{i,\text{GENERIC MC}} - R_{i,\text{NEMD}})/R_{i,\text{NEMD}}]^2}{\sum_{i=1}^{n_{\text{type}}} w_i}}, \tag{27}$$

i.e., as the root mean square of the differences between GENERIC MC and NEMD data for $\tilde{\mathbf{c}}$, becomes zero within some tolerance. In Eq. (27), n_{type} denotes the number of data types, w_i is a weighting factor, and R denotes the value for $\tilde{\mathbf{c}}$ obtained either from the GENERIC MC or the NEMD simulation. Since α_{zz} has been assumed to be zero, $\tilde{c}_{zz}$ (which is mostly controlled by α_{zz}) can be relegated from the objective function; thus, n_{type} is set equal to three ($\tilde{c}_{xx}$, $\tilde{c}_{xy}$, and $\tilde{c}_{yy}$). Furthermore, we chose to put the same weight on each of $\tilde{c}_{xx}$, $\tilde{c}_{xy}$, and $\tilde{c}_{yy}$, implying that $w(\tilde{c}_{xy})=w(\tilde{c}_{xx})=w(\tilde{c}_{yy})$. However, one is free to choose a different way of weighting, depending on his/her own physical viewpoint and intuition; for example, if one considers the shear viscosity to be a more important property than the two normal stress coefficients, a reasonable choice will be $w(\tilde{c}_{xy})>w(\tilde{c}_{xx})>w(\tilde{c}_{yy})$.

Step (4): At convergence, the micro- and macrosolvers will have been consistently bridged with each other through a macroscopic model with a number of important consequences: (1) Knowing the relationship $\boldsymbol{\alpha}=\boldsymbol{\alpha}(\dot{\gamma})$ is practically equivalent to having computed the free energy A of the system with respect to the equilibrium (zero-flow) state. (2) One can validate or evaluate (and thus exclude) specific macroscopic models if their predictions for the tensor $\boldsymbol{\alpha}$ deviate significantly from the obtained $\boldsymbol{\alpha}=\boldsymbol{\alpha}(\dot{\gamma})$ relationship of the coupled micro-macro model computations. (3) The computed $\boldsymbol{\alpha}=\boldsymbol{\alpha}(\dot{\gamma})$ relationship can serve as a starting point in order to propose more accurate viscoelastic models. For example, as we will see below, the choice $\alpha_{zz}=0$ is not entirely correct, since the results for the zz component of the conformation tensor from the GENERIC MC simulations could not be matched with those from the micromodel. (4) By studying the dependence of $\boldsymbol{\alpha}$ on the chemical or architectural details of the simulated polymer melt, one can understand how chemical composition affects viscoelastic response. (5) By studying the dependence of $\boldsymbol{\alpha}$ on chain length N, one can obtain the relationship $\boldsymbol{\alpha}=\boldsymbol{\alpha}(\dot{\gamma};N)$; by extrapolating then to longer N's, one could study higher molecular weight polymers, for which the direct application of the NEMD model is impossible due to the problem of long relaxation times. In contrast, the macromodel does not suffer from any such shortcomings. Indeed, a theoretical analysis of the structural-conformational changes induced by chain connectivity MC moves has shown that[44] their efficiency increases with increasing chain length. This is in contrast to conventional brute-force dynamic methods which all suffer from the problem of long relaxation times, namely, the rapid increase in the longest relaxation time of the polymer with chain length. Fast equilibration also implies that one can use this solver to interpolate over an expanded domain of phase points and then project. For example, in the present work, we have been able to analyze the dependence of the tensor $\boldsymbol{\alpha}$ on the chain length of the simulated polymer melt. This, in the future, can be used as a guide to compute its values for longer chain length systems of the same polymer. It opens therefore the way to executing reliable GENERIC MC simulations in regimes completely inaccessible today by dynamic microscopic models. This can help obtain the viscoelastic properties of polymers of relevance to industrial practice. Work along this direction is already in progress.

A few other remarks about the proposed methodology are in place here:

(i) Given that the Lagrange multipliers are related to the velocity gradients in a homogeneous steady flow, their calculation is equivalent to computing the elements (or certain blocks) of the friction matrix $\mathbf{M}$ of the macroscopic GENERIC model, which usually has a blocklike structure.[30] Combined with the results of some additional direct dynamic simulations and the use of the Green-Kubo formulae,[12,40,45,46] one then can hope to compute all subblocks of $\mathbf{M}$.

(ii) Although we outlined the method for the case of a tensorial structural variable (the conformation tensor $\tilde{\mathbf{c}}$), the entire methodology is equally applicable if the structural variable is, e.g., a distribution function, which is the case for entangled polymers. Guided from the reptation theory, one can attempt a description of these systems in homogeneous time-independent flows, in terms of the probability density function $f(\mathbf{u},s)$ expressing the distribution of the tangent unit vector $\mathbf{u}$ along the contour of the primitive path of the reptating chain at position s along its contour.[47] The orientation vector $\mathbf{u}$ will be a property of a smoothed chain obtained by reducing atomistic chains to primitive paths.[48–50]

(iii) The macroscale model can serve not only to parametrize the macroscopic model but also to correct the functional form of its building blocks (referring to, e.g., the free energy A and the friction matrix $\mathbf{M}$). We provide an example below.

III. APPLICATION

A. Systems studied and simulation details

We have studied three different unentangled linear polyethylene (PE) melts ($C_{50}H_{102}$, $C_{78}H_{158}$, and $C_{128}H_{258}$) at T

=450 K corresponding to the following density values: ρ =0.7426 g/cm^3 for the $C_{50}H_{102}$ system, ρ=0.7638 g/cm^3 for the $C_{78}H_{158}$ system, and ρ=0.7754 g/cm^3 for the $C_{128}H_{258}$ system. Five or six different nonequilibrium states covering a broad range of De numbers were selected for each system, spanning both the linear and the nonlinear viscoelastic regimes: $0.5 \leq De \leq 130$ for the $C_{50}H_{102}$ system ($\lambda_0 = 0.56 \pm 0.03$ ns, as estimated by the time integral of the stretched-exponential curve describing the autocorrelation function for the chain end-to-end vector), $0.9 \leq De \leq 800$ for the $C_{78}H_{158}$ system ($\lambda_0 = 2.3 \pm 0.2$ ns), and $0.6 \leq De \leq 700$ for the $C_{128}H_{258}$ system ($\lambda_0 = 8.0 \pm 0.6$ ns). To avoid any undesirable system-size effects (especially at the higher De numbers studied), large rectangular boxes (enlarged in the flow direction) were employed in all cases based on the following data for the size R_{max} of a fully stretched chain length (i.e., with the equilibrium bond length and bending angle in the all *trans*-conformation)[13] and the mean chain end-to-end distance at equilibrium $\langle R^2 \rangle_{eq}^{1/2}$ in each one of them: R_{max} =63.3 Å and $\langle R^2 \rangle_{eq}^{1/2} = 29.7 \pm 0.3$ Å for the $C_{50}H_{102}$ system, R_{max}=99.4 Å and $\langle R^2 \rangle_{eq}^{1/2} = 38.6 \pm 0.4$ Å for the $C_{78}H_{158}$ system, and R_{max}=164 Å and $\langle R^2 \rangle_{eq}^{1/2} = 50.7 \pm 0.4$ Å for the $C_{128}H_{258}$ system. More specifically, if x, y, and z denote the flow, velocity gradient, and neutral directions, respectively, the box dimensions ($x \times y \times z$ in units of angstroms) were set equal to $93.02 \times 45 \times 45$ Å^3 for the $C_{50}H_{102}$ melt (it contained 120 chains), equal to $130.5 \times 54 \times 54$ Å^3 for the $C_{78}H_{158}$ melt (it contained 160 chains), and equal to $212.7 \times 68 \times 68$ Å^3 for the $C_{128}H_{258}$ melt (it contained 256 chains). Thus, the x dimension of the simulation box in each system was at least 30% larger than its R_{max} value, and similarly for the y and z dimensions based on the corresponding $\langle R^2 \rangle_{eq}^{1/2}$ data.

For both sets of simulations (GENERIC MC and NEMD), the Siepmann-Karaboni-Smit united-atom potential model[67] was employed, with the exception of a harmonic flexible bond-stretching potential adopted in the NEMD simulations.[68] The equations of motion in the NEMD method were integrated with the *r*-RESPA (reversible reference system propagator algorithm),[69] by utilizing two different time steps: 2.35 fs for the integration of the slow-varying forces (corresponding to the nonbonded Lennard-Jones interactions, the Nosé-Hoover thermostat,[62,63] and the flow field), and 0.47 fs for the integration of the fast-varying ones (corresponding to bond-stretching, bond-bending, and bond-torsional interactions).

The efficient chain-connectivity altering end-bridging move[44] was employed for the GENERIC MC simulations allowing for a small polydispersity $I \approx 1.083$ with a uniform chain-length distribution in all systems. If polydispersity is to be suppressed, the end-bridging moves should be replaced by double bridging ones.[70]

B. Results and discussion

1. Synthetic nonequilibrium thermodynamic field

In Fig. 1, we present our results for the nonzero values of the thermodynamic field $\boldsymbol{\alpha}$, as a function of the De number for the three systems. As seen, for all systems, α_{xx} and α_{xy}

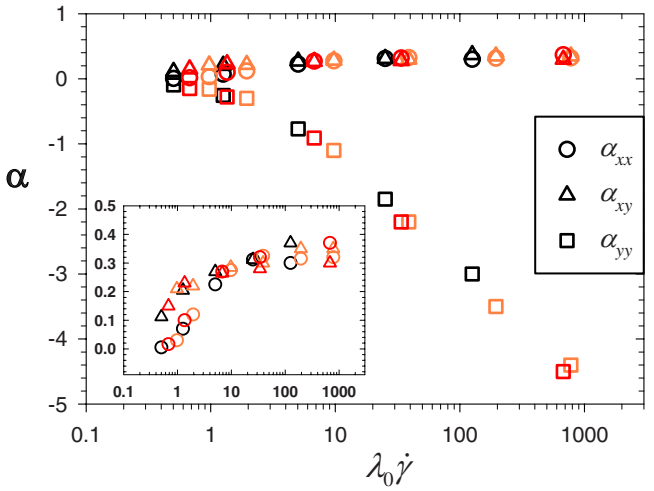

FIG. 1. (Color online) Variation in the thermodynamic force field (Lagrange multiplier) $\boldsymbol{\alpha}$ with De for the three PE melts: black symbols refer to $C_{50}H_{102}$, orange (light gray) symbols to $C_{78}H_{158}$, and red (dark gray) symbols to $C_{128}H_{258}$.

increase monotonically with increasing De. In fact, at low De numbers, α_{xx} appears to be smaller than α_{xy} in magnitude (see inset); this is considered to be consistent with our physical intuition that, at small flow fields, chains tend to be oriented in the direction of the flow without distorting their overall shape. At higher De numbers (e.g., $De \geq 100$), both quantities are observed to attain plateau values; this represents the saturation of the overall chain conformation which, in conjunction with dynamical mechanisms such as rotation or tumbling, precludes chains from obtaining their fully stretched configuration in shear. Here, it should be noted that, by nature, GENERIC MC cannot address tumbling; however, as we will see shortly (see Fig. 2 below), the method is capable of effectively generating a structure for the physical system at nonequilibrium states which overall is similar to that obtained by NEMD, which is the most important in determining the structural and rheological properties of dense liquid systems.

In contrast to α_{xx} and α_{xy}, α_{yy} is found to attain negative values whose absolute magnitude is considerably larger than those of α_{xx} and α_{xy} for practically all De numbers studied, as clearly seen in Fig. 1. This reflects the fact that the y dimension of the overall shape of a chain becomes smaller than its equilibrium value due to alignment and stretching along the flow (x) direction. An interesting point to observe is that all components of $\boldsymbol{\alpha}$ are rather insensitive to the chain length in the whole range of De. This is considered as a very promising aspect of the GENERIC MC method in practical applications, since one can utilize results from (the computationally cheaper) simulations with shorter-chain systems to obtain reasonable *a priori* guesses for $\boldsymbol{\alpha}$ for (the computationally more expensive) simulations with longer-chain systems. (Using the relationship $\boldsymbol{\alpha}$ vs. De obtained from the present simulations with shorter PE systems, we are currently exploiting such an approach to simulate a longer PE melt, $C_{400}H_{802}$.) More importantly, the $\boldsymbol{\alpha}$-vs.-De plots obtained from the proposed methodology can be used to calculate "realistic" free energies at various nonequilibrium states

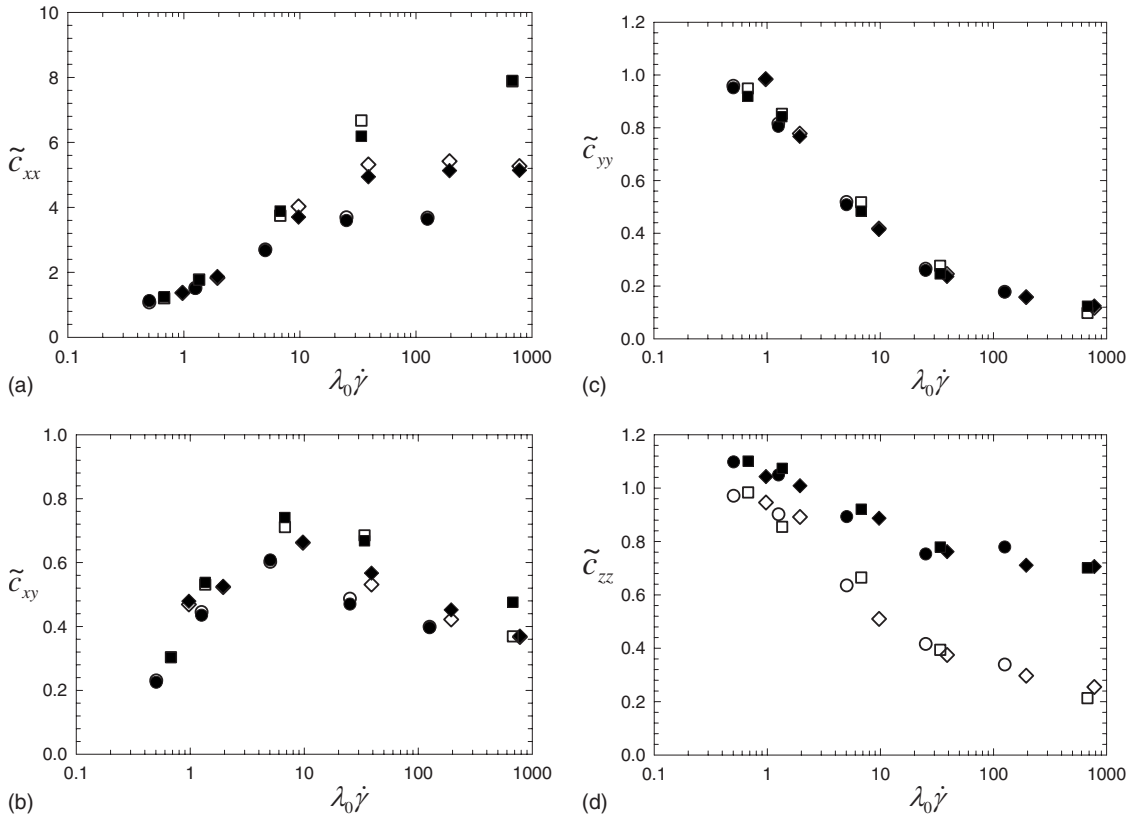

FIG. 2. Comparison of the xx, xy, yy, and zz components of the conformation tensor $\tilde{\mathbf{c}}$ between NEMD and GENERIC MC, as a function of the De number for the three simulated PE melts: $C_{50}H_{102}$ (circles), $C_{78}H_{158}$ (diamonds), and $C_{128}H_{258}$ (squares). Filled symbols represent the GENERIC MC data and open ones the NEMD data. The error bars are commensurate with the size of the symbols.

through, e.g., a step-by-step thermodynamic integration of Eq. (17a). This, in turn, can be exploited in order to compute important thermodynamic quantities (e.g., the configurational entropy and nonequilibrium heat capacities) or to verify fundamental thermodynamic relationships for nonequilibrium systems (e.g., the Maxwell relations[56] referring to nonequilibrium structural variables).

2. Conformation tensor

In Fig. 2, we compare the values of $\tilde{\mathbf{c}}$ obtained for each system from the two methods (GENERIC MC, using the $\boldsymbol{\alpha}$ values shown in Fig. 1, and direct NEMD). For all state points considered, excellent agreement between the two methods is observed for $\tilde{c}_{xx}$, $\tilde{c}_{xy}$, and $\tilde{c}_{yy}$. These results can be used next to get estimates of the material functions of the simulated polymers in shear (i.e., the shear viscosity and the first normal stress coefficient), through the well-known linear relationship between $\tilde{\mathbf{c}}$ and the extra stress tensor $\boldsymbol{\tau}$ based on the network theory,[8,10] see also Eq. (12). It is only for the $\tilde{c}_{zz}$ component of the conformation tensor that the agreement between the two methods is rather poor, for all three systems. This result is attributed to the zero value assumed for the zz component for $\boldsymbol{\alpha}$ proposed by a number of currently available viscoelastic models. It suggests therefore a need for modification. Since $\tilde{c}_{zz}$ and $\tilde{c}_{yy}$ are directly related with the second normal stress coefficient, this deviation also explains why many of the constitutive differential equations of the category of conformation tensor models fail to provide a satisfactory description of rheological data for this important material function. As demonstrated in Appendix A, the reduction $\alpha_{zz}=0$ cannot be avoided even if one incorporates higher-order terms in the expansion of the free-energy functional with respect to the conformation tensor, as long as $f_3=f_4=0$ in Eq. (14).[71] It is only through the f_3 and f_4 terms (i.e., through different combinations of $\tilde{\mathbf{c}}$) that nonzero α_{zz} values can be obtained without violating the Onsager-Casimir reciprocity principles or the second law of thermodynamics. We discuss this issue in Appendixes A and B.

3. Orientation angle

We turn now to a more stringent test of the GENERIC MC method, namely, its capability to capture structural details at the level of internal segments along the chain and how these compare with the results obtained from the micromodel (the NEMD simulations). To this, in Fig. 3, we compare the values of the orientation angle χ obtained from the two methods. χ is a quantity that can be determined by flow birefringence and refers to the anisotropy in the bond orientation along the polymer chains due to the applied flow field (form birefringence is neglected in homogeneous melt systems).[72] Overall, the agreement is very good at all state

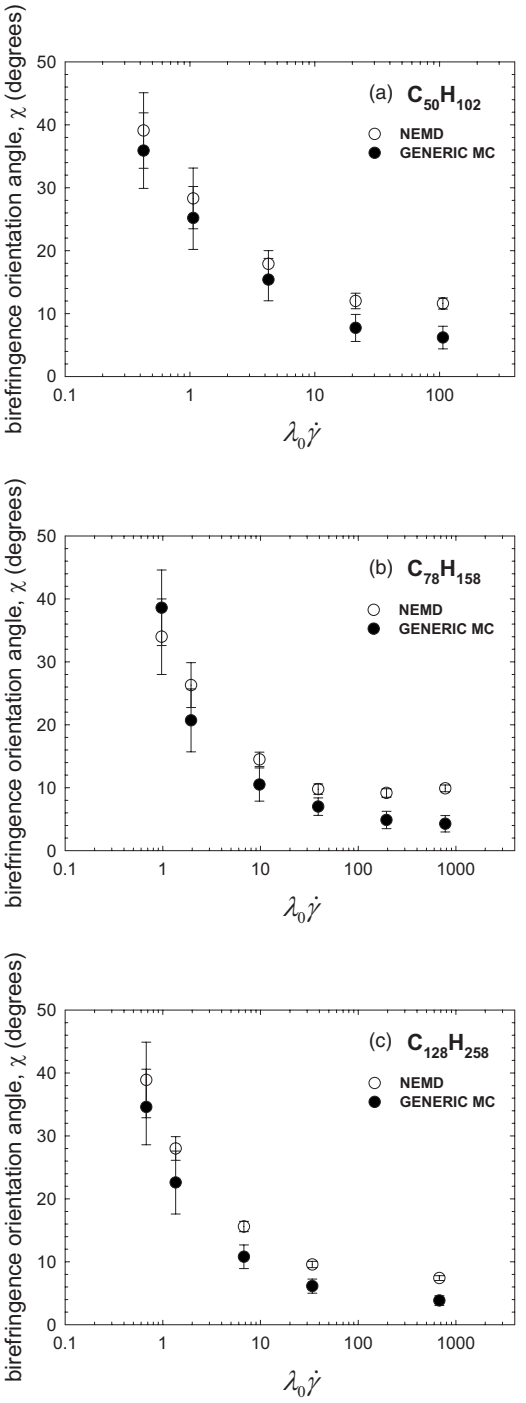

FIG. 3. Comparison of the birefringence orientation (or extinction) angle χ between NEMD and GENERIC MC, at various shear rates for (a) the $C_{50}H_{102}$, (b) the $C_{78}H_{158}$, and (c) the $C_{128}H_{258}$ PE melts. χ represents the angle between the flow direction and the direction of the eigenvector corresponding to the largest eigenvalue of the birefringence tensor.

points, especially for De numbers less than about 10. This should be interpreted as an excellent performance of the GENERIC MC method (the macrosolver), considering especially that it aimed at capturing flow effects through the use of just only one (the longest) mode (the chain end-to-end tensor $\tilde{\mathbf{c}}$).

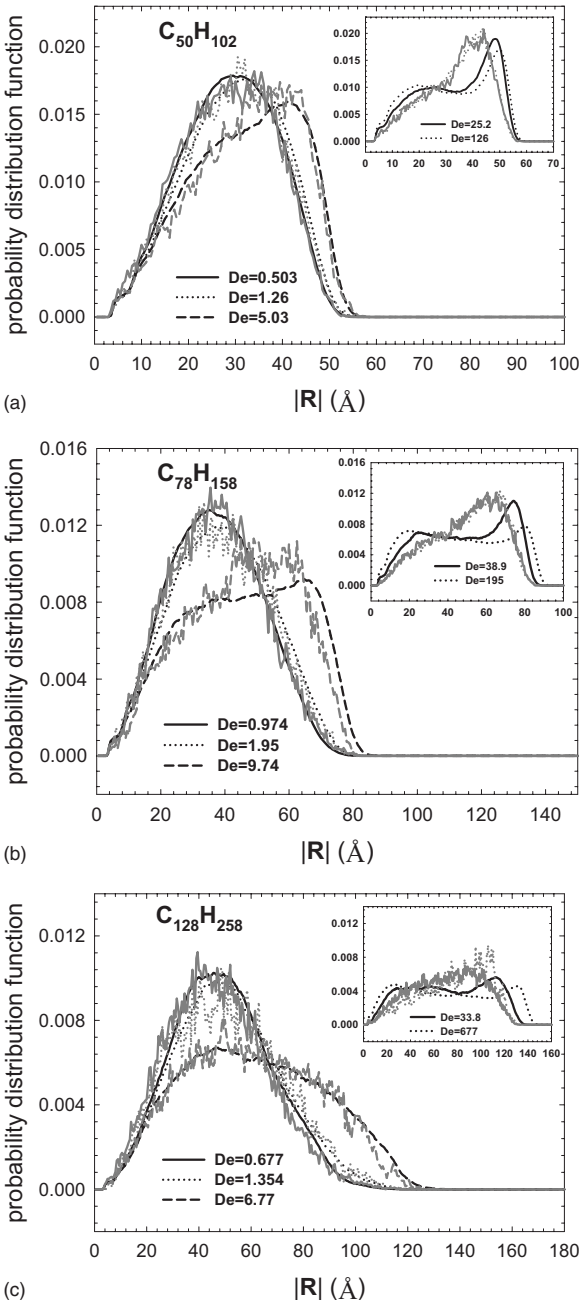

FIG. 4. Comparison between NEMD (black lines) and GENERIC MC (gray lines) results for the end-to-end distance $|\mathbf{R}|$ probability distribution function, at various De numbers, for (a) the $C_{50}H_{102}$, (b) the $C_{78}H_{158}$, and (c) the $C_{128}H_{258}$ systems. Deviations from the Gaussian behavior are observed at De numbers approximately larger than about 2 in all systems. For clarity, the results at these higher De numbers are shown separately in the inset.

4. Distribution of the chain end-to-end vector

Another interesting comparison between NEMD and GENERIC MC simulations is shown in Figs. 4 and 5. Figure 4 compares the probability distribution function for the chain end-to-end distance $|\mathbf{R}|$ in the two models for the three systems, at various De numbers. At low De values, the resulting distributions are Gaussian in the two cases and compare very favorably with each other. As the value of De increases

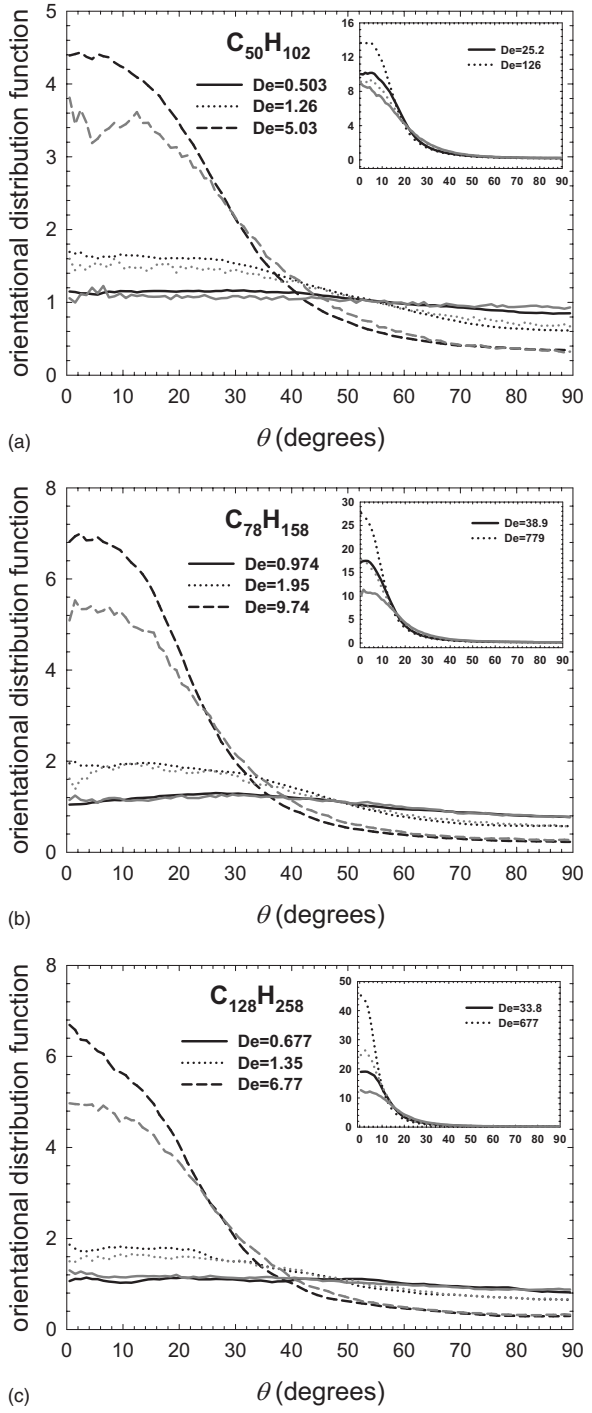

FIG. 5. Comparison between NEMD (black lines) and GENERIC MC (gray lines) results for the distribution function of the orientation angle θ (apart from a sin θ term corresponding to the Jacobian of the transformation to polar coordinates) of the chain end-to-end vector with respect to the flow direction, for (a) the $C_{50}H_{102}$, (b) the $C_{78}H_{158}$, and (c) the $C_{128}H_{258}$ systems. For clarity, the results at the higher De numbers are shown also separately in the inset.

above approximately 2, the two distributions exhibit deviations from the Gaussian behavior; interestingly enough, the GENERIC MC simulations can capture this behavior both qualitatively and quantitatively even outside the linear regime (up to De numbers approximately equal to 10 in all systems). It is only for De $\geq$ 10 (see insets) that systematic deviations between the two methods become obvious. A particularly noticeable phenomenon there is the appearance of two peaks (one at low $|\mathbf{R}|$ and another at high $|\mathbf{R}|$ values) in the NEMD plots at these high De numbers (instead of one observed at lower De ones). The GENERIC MC simulations cannot capture this: they continue to predict only a single peak at the high $|\mathbf{R}|$ values. Given that the peak at low $|\mathbf{R}|$ values is a consequence of chain rotation or tumbling due to the rotational character of shear, this deviation reflects the inherent inability of the (nondynamic) GENERIC MC method to directly accommodate any dynamic (i.e., momentum) information. Despite this, however, it is encouraging that the GENERIC MC simulations are capable of qualitatively following the overall behavior observed in the NEMD simulations even at high De numbers: for example, they can capture the extended region of the distribution at intermediate $|\mathbf{R}|$ values [this is more pronounced in the results of Fig. 4(c) for the $C_{128}H_{258}$ system], which shows up in the NEMD plots.

5. Distribution of the chain orientation angle

Figure 5 extends the comparison between the two methods at the level of the distribution function for the orientation angle θ of the chain end-to-end vector with respect to the flow direction. At equilibrium, chains are directed isotropically in space and therefore the distribution function is uniform (up to a mathematical sin θ term related to the Jacobian of the distribution). Upon increasing the flow field, however, the chains become more and more aligned along the flow direction, which results in higher populations at the smaller θ values; this is clearly observed in the figure. Again, very good agreement is observed between GENERIC MC and NEMD, especially for De $\leq$ 10, in all systems. Beyond De $\approx$ 10 (see inset), quantitative deviations are noticed between the two simulation sets, although, qualitatively, the trends are similar.

6. Symmetry of the stress tensor

An important relationship between $\boldsymbol{\alpha}$ and $\tilde{\mathbf{c}}$ can be derived based on the GENERIC (Ref. 12) or generalized bracket formalism[10] for the elastic stress. Indeed, according to Eqs. (12) and (19), and taking into account the symmetry property of the stress tensor and the kinematics of the shear flow, one obtains[41]

$$\frac{\alpha_{xx} - \alpha_{yy}}{\alpha_{xy}} = \frac{\tilde{c}_{xx} - \tilde{c}_{yy}}{\tilde{c}_{xy}}. \tag{28}$$

The curves of Fig. 6, where all the results of the present GENERIC MC simulations have been collected, reveal excellent agreement of the simulation findings with Eq. (28) at all state points, further justifying the correctness of the proposed GENERIC MC methodology and the robustness of the coupled micro-macro computations pursued in this work.

IV. CONCLUSIONS, FUTURE PLANS, OUTLOOK

We have described a framework for the multiscale modeling of polymer viscoelasticiy, in which the physics is

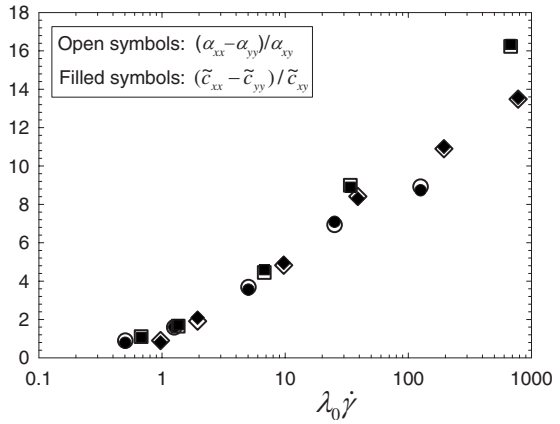

FIG. 6. $(\alpha_{xx}-\alpha_{yy})/\alpha_{xy}$ versus $(\tilde{c}_{xx}-\tilde{c}_{yy})/\tilde{c}_{xy}$, as a function of shear rate in the three simulated PE melts: $C_{50}H_{102}$ (circles), $C_{78}H_{158}$ (diamonds), and $C_{128}H_{258}$ (squares).

known at a microscopic level but the needed data refer to a higher, coarse-grained macroscopic level. The basic idea is to represent the macroscopic model by using a nondynamic method that generates nonequilibrium states of the physical systems in an expanded statistical ensemble designed to incorporate synthetic field variables. For a given value of the imposed shear rate, the synthetic fields are determined iteratively so that the solutions of the micro- and macrosolvers for the coarse-grained structural variables coincide. The biggest advantage of the present methodology is that the macrosolver proceeds without knowing *a priori* the exact form of the macroscopic model. Guided by the GENERIC framework of nonequilibrium thermodynamics, it relies solely on the nature of the structural variables chosen to represent the system at a coarser level.

We have demonstrated the applicability of the method in the case of short-chain length (i.e., unentangled) polymer melts, for which the appropriate structural variable to consider is the chain end-to-end conformation tensor. But, conceptually, the method can be straightforwardly extended to models and/or physical systems described by other variables, such as a configuration tensor and a scalar (this is the case of long chain branched polymers) or a distribution function (this is the case of entangled polymer melts).[12]

From a technical point of view, the main tool is a very efficient MC algorithm which can be executed in an expanded statistical ensemble. Based on a set of extremely efficient moves (such as end-bridging and double-bridging), this algorithm can easily bypass huge free energy barriers separating different phase-space points in polymeric fluids and drive them to certain nonequilibrium steady states (for a given flow field) considerably faster than with any conventional MD or constrained MD simulation. This feature is particularly attractive for systems (such as high molecular weight polymers) characterized by relaxation times orders of magnitude higher than what can be simulated today with a brute-force dynamic method. On the other hand, the time to reach nonequilibrium steady states by GENERIC MC appears to be relatively insensitive to the magnitude of the applied strain rate, in contrast to NEMD simulations where the corresponding time depends strongly on the imposed strain rate (usually the smaller the applied strain rate, the longer the simulation time[58,68]). Based on this, a possible practical use of the present simulation framework to long polymer systems is to apply first GENERIC MC to drive the system in the neighborhood of a target nonequilibrium state (for a given shear rate), and then turn to NEMD to sample phase-space points and compute all the needed dynamic information. If necessary, some intermediate GENERIC MC runs can be performed to move the system more rapidly in phase space.

GENERIC MC can also be used to calculate the fundamental thermodynamic functions of nonequilibrium polymeric systems under flow through thermodynamic integration; see Eqs. (17a), (17b), (18), and (19). This would enable the macrosolver to compute significant thermodynamic properties of flowing polymers (e.g., nonequilibrium heat capacities).[73]

Although the current GENERIC MC methodology has been developed for atomistic-level simulations, the basic idea (i.e., expanding the statistical ensemble to include appropriate structural variables whose conjugate fields can account for flow effects) is readily extendable to coarser-level simulators and methodologies such as those relying on atom-lumping methods[52,74] and self-consistent field schemes.[75,76]

By far, however, the most important feature of the proposed methodology is the opportunity it offers for improved constitutive modeling. For example, for the family of conformation tensor models discussed here, that the zz component of the tensor $\boldsymbol{\alpha}$ should not be zero invalidates or puts question marks next to a number of well-known and widely used phenomenological constitutive equations. Simultaneously, it holds the promise of correcting these models (for more accurate engineering applications); for the problem at hand, most of this hope comes from the "simulations-assisted" improvements that can be expected for the relaxation matrix $\boldsymbol{\Lambda}$ (see, for example, Appendix B) describing dissipative effects in the macroscopic equation.

Currently, efforts are in progress to extend the methodology to the case of entangled polymers by using multiple conformation tensors based on topological measures that can identify entanglements along the chain contour and by taking the entanglement strands as the active stress segments at the coarse level. Alternatively, inspired by the Doi-Edwards reptation model,[47] one can resort to a description in terms of the orientational distribution function $f(\mathbf{u},s)$ representing the probability that the unit end-to-end vector of the entanglement segment s along the chain is equal to $\mathbf{u}$ (within $d\mathbf{u}$).

ACKNOWLEDGMENTS

We feel deeply indebted to Dow Benelux B. V. (especially to Joey Storer, Jaap den Doelder, and Rudy Koopmans) for financial support and for their genuine interest in this work. We are also grateful to Antony Beris, Hans Christian Öttinger, Doros Theodorou, and Ioannis Kevrekidis for many helpful discussions.

APPENDIX A: PROOF OF $\alpha_{zz}=0$ FOR THE CASE OF Λ GIVEN BY Eq. (14) WITH $f_3=f_4=0$

In this appendix, we first show that an expression for the relaxation matrix of the form of Eq. (14) with $f_3=f_4=0$, i.e.,

$$\Lambda_{\alpha\beta\gamma\varepsilon}(\tilde{\mathbf{c}}) = f_1(I_1)(\tilde{c}_{\alpha\gamma}\delta_{\beta\varepsilon} + \tilde{c}_{\alpha\varepsilon}\delta_{\beta\gamma} + \tilde{c}_{\beta\gamma}\delta_{\alpha\varepsilon} + \tilde{c}_{\beta\varepsilon}\delta_{\alpha\gamma}) + 2f_2(I_1)(\tilde{c}_{\alpha\gamma}\tilde{c}_{\beta\varepsilon} + \tilde{c}_{\alpha\varepsilon}\tilde{c}_{\beta\gamma}), \tag{A1}$$

together with a free-energy function A representing a general FENE spring [see Eq. (A6) below], leads to $\alpha_{zz}=0$ in the case of steady shear. Indeed, solving Eq. (11) for the zz component of $\tilde{\mathbf{c}}$ for the flow described by Eq. (20), we get

$$\hat{\tilde{c}}_{zz} = -nk_BT(\Lambda_{zzxx}\alpha_{xx} + 2\Lambda_{zzxy}\alpha_{xy} + \Lambda_{zzyy}\alpha_{yy} + \Lambda_{zzzz}\alpha_{zz}) = 0. \tag{A2}$$

From Eq. (A1), on the other hand, it is also found that

$$\Lambda_{zzxx} = \Lambda_{zzxy} = \Lambda_{zzyy} = 0, \quad \Lambda_{zzzz} = (f_1\tilde{c}_{zz} + f_2\tilde{c}_{zz}^2). \tag{A3}$$

Substituting then Eq. (A3) into Eq. (A2) yields

$$(f_1\tilde{c}_{zz} + f_2\tilde{c}_{zz}^2)\alpha_{zz} = 0. \tag{A4}$$

Now, let us consider the range of admissible values for the functions f_1 and f_2 for which the second law of thermodynamics is not violated. This is equivalent to requiring[10]

$$\frac{\delta A^*}{\delta\tilde{c}_{\alpha\beta}}\Lambda_{\alpha\beta\gamma\varepsilon}\frac{\delta A^*}{\delta\tilde{c}_{\gamma\varepsilon}} \geq 0 \tag{A5}$$

representing a non-negative rate of entropy production by the degradation of mechanical energy. The normalized (by nk_BT) free energy A^* for a general nonlinear FENE spring can be written as

$$A^*(\tilde{\mathbf{c}}) = \int \frac{1}{2}[\phi(\mathrm{tr}\,\tilde{\mathbf{c}}) - \ln(\det|\tilde{\mathbf{c}}|)]d^3x = \int \frac{1}{2}[\phi(I_1) - \ln(I_3)]d^3x, \tag{A6}$$

where I_3 is the determinant of $\tilde{\mathbf{c}}$ and ϕ an arbitrary function of I_1. Differentiating A^* with respect to $\tilde{\mathbf{c}}$ gives

$$\frac{\delta A^*}{\delta\tilde{c}_{\alpha\beta}} = \frac{1}{2}[h_1(I_1)\delta_{\alpha\beta} - \tilde{c}^{-1}_{\alpha\beta}], \tag{A7}$$

where $h_1(I_1) = \frac{\delta A^*}{\delta I_1} = \frac{\partial\phi}{\partial I_1}$, while $\tilde{\mathbf{c}}^{-1}$ denotes the inverse of $\tilde{\mathbf{c}}$. Multiplication of Eq. (A1) by Eq. (A7) results in

$$\Lambda_{\alpha\beta\gamma\varepsilon}\frac{\delta A^*}{\delta\tilde{c}_{\gamma\varepsilon}} = 2f_1(I_1)[h(I_1)\tilde{c}_{\alpha\beta} - \delta_{\alpha\beta}] + 2f_2(I_1)[h(I_1)\tilde{c}_{\alpha\gamma}\tilde{c}_{\gamma\beta} - \tilde{c}_{\alpha\beta}]. \tag{A8}$$

Then, multiplying Eq. (A8) by Eq. (A7) (and after some mathematical operations) leads to

$$\begin{aligned}\frac{\delta A}{\delta\tilde{c}_{\alpha\beta}}\Lambda_{\alpha\beta\gamma\varepsilon}\frac{\delta A}{\delta\tilde{c}_{\gamma\varepsilon}} &= [h\delta_{\alpha\beta} - \tilde{c}^{-1}_{\alpha\beta}]\{f_1(I_1)[h\tilde{c}_{\alpha\beta} - \delta_{\alpha\beta}] + f_2(I_1) \times [h\tilde{c}_{\alpha\gamma}\tilde{c}_{\gamma\beta} - \tilde{c}_{\alpha\beta}]\} \\ &= f_1(I_1)[h^2\,\mathrm{tr}(\tilde{\mathbf{c}}) - 6h + \mathrm{tr}(\tilde{\mathbf{c}}^{-1})] + f_2(I_1) \times [h\,\mathrm{tr}(\tilde{\mathbf{c}}\cdot\tilde{\mathbf{c}}) - 2h\,\mathrm{tr}(\tilde{\mathbf{c}}) + 3] \\ &= \sum_{i=1}^{3}[f_1(I_1)(h^2\lambda_i - 2h + \lambda_i^{-1}) + f_2(I_1)(h^2\lambda_i^2 - 2h\lambda_i + 1)] \\ &= \sum_{i=1}^{3}\frac{1}{\lambda_i}(h\lambda_i - 1)^2[f_1(I_1) + f_2(I_1)\lambda_i],\end{aligned} \tag{A9}$$

where the λ_i's are the eigenvalues of $\tilde{\mathbf{c}}$ in three-dimensional space; we have also used that $\mathrm{tr}(\tilde{\mathbf{c}}) = \Sigma_{i=1}^3\lambda_i$ and $\mathrm{tr}(\tilde{\mathbf{c}}\cdot\tilde{\mathbf{c}}) = \Sigma_{i=1}^3\lambda_i^2$ [more generally, $\mathrm{tr}(\overbrace{\tilde{\mathbf{c}}\cdot\tilde{\mathbf{c}}\cdots\tilde{\mathbf{c}}}^{n}) = \Sigma_{i=1}^3\lambda_i^n$]. Since $\tilde{\mathbf{c}}$ is positive definite by definition [see Eq. (10)], all λ_i's must be positive. Hence, a sufficient condition for inequality (A5) to be satisfied is

$$f_1(I_1) \geq 0 \ \text{ and } \ f_2(I_1) \geq 0. \tag{A10}$$

Combining Eq. (A4) with Eq. (A10), we finally arrive at $\alpha_{zz}=0$.

That α_{zz} should be zero for Eq. (A1) is also found even if one considers a more general form for $\mathbf{\Lambda}$ by allowing for higher-order terms in $\tilde{\mathbf{c}}$ while maintaining the symmetric structure in the permutation of indices α, β, γ, and ε implied by Eq. (A1), namely,

$$A_{\alpha\gamma}B_{\beta\varepsilon} + A_{\alpha\varepsilon}B_{\beta\gamma} + A_{\beta\gamma}B_{\alpha\varepsilon} + A_{\beta\varepsilon}B_{\alpha\gamma} \text{ for two different second-rank objects.} \tag{A11}$$

It is important to recognize that this structure satisfies the Onsager symmetry properties required for $\mathbf{\Lambda}$:

$$\Lambda_{\alpha\beta\gamma\varepsilon} = \Lambda_{\gamma\varepsilon\alpha\beta} = \Lambda_{\beta\alpha\gamma\varepsilon} = \Lambda_{\beta\alpha\varepsilon\gamma}. \tag{A12}$$

Making use of the symmetry properties of Eq. (A11), the more general form of Eq. (A1) for $\mathbf{\Lambda}$ is then derived to be

$$\begin{aligned}\Lambda_{\alpha\beta\gamma\varepsilon}(\tilde{\mathbf{c}}) = {} & f_1(I_1)(\tilde{c}_{\alpha\gamma}\delta_{\beta\varepsilon} + \tilde{c}_{\alpha\varepsilon}\delta_{\beta\gamma} + \tilde{c}_{\beta\gamma}\delta_{\alpha\varepsilon} + \tilde{c}_{\beta\varepsilon}\delta_{\alpha\gamma}) + 2f_2(I_1)(\tilde{c}_{\alpha\gamma}\tilde{c}_{\beta\varepsilon} + \tilde{c}_{\alpha\varepsilon}\tilde{c}_{\beta\gamma}) + f_3(I_1)(\tilde{c}_{\alpha\gamma}\tilde{c}_{\beta\eta}\tilde{c}_{\eta\varepsilon} + \tilde{c}_{\alpha\varepsilon}\tilde{c}_{\beta\eta}\tilde{c}_{\eta\gamma} + \tilde{c}_{\beta\gamma}\tilde{c}_{\alpha\eta}\tilde{c}_{\eta\varepsilon} \\ & + \tilde{c}_{\beta\varepsilon}\tilde{c}_{\alpha\eta}\tilde{c}_{\eta\gamma}) + 2f_4'(I_1)(\tilde{c}_{\alpha\sigma}\tilde{c}_{\sigma\gamma}\tilde{c}_{\beta\eta}\tilde{c}_{\eta\varepsilon} + \tilde{c}_{\alpha\sigma}\tilde{c}_{\sigma\varepsilon}\tilde{c}_{\beta\eta}\tilde{c}_{\eta\gamma}) + f_4''(I_1)(\tilde{c}_{\alpha\gamma}\tilde{c}_{\beta\sigma}\tilde{c}_{\sigma\eta}\tilde{c}_{\eta\varepsilon} + \tilde{c}_{\alpha\varepsilon}\tilde{c}_{\beta\sigma}\tilde{c}_{\sigma\eta}\tilde{c}_{\eta\gamma} + \tilde{c}_{\beta\gamma}\tilde{c}_{\alpha\sigma}\tilde{c}_{\sigma\eta}\tilde{c}_{\eta\varepsilon} \\ & + \tilde{c}_{\beta\varepsilon}\tilde{c}_{\alpha\sigma}\tilde{c}_{\sigma\eta}\tilde{c}_{\eta\gamma}) + f_5'(I_1)(\tilde{c}_{\alpha\sigma}\tilde{c}_{\sigma\gamma}\tilde{c}_{\beta\sigma}\tilde{c}_{\sigma\eta}\tilde{c}_{\eta\varepsilon} + \tilde{c}_{\alpha\sigma}\tilde{c}_{\sigma\varepsilon}\tilde{c}_{\beta\sigma}\tilde{c}_{\sigma\eta}\tilde{c}_{\eta\gamma} + \tilde{c}_{\beta\sigma}\tilde{c}_{\sigma\gamma}\tilde{c}_{\alpha\sigma}\tilde{c}_{\sigma\eta}\tilde{c}_{\eta\varepsilon} + \tilde{c}_{\beta\sigma}\tilde{c}_{\sigma\varepsilon}\tilde{c}_{\alpha\sigma}\tilde{c}_{\sigma\eta}\tilde{c}_{\eta\gamma}) \\ & + f_5''(I_1)(\tilde{c}_{\alpha\gamma}\tilde{c}_{\beta\sigma}\tilde{c}_{\sigma\eta}\tilde{c}_{\eta\mu}\tilde{c}_{\mu\varepsilon} + \tilde{c}_{\alpha\varepsilon}\tilde{c}_{\beta\sigma}\tilde{c}_{\sigma\eta}\tilde{c}_{\eta\mu}\tilde{c}_{\mu\gamma} + \tilde{c}_{\beta\gamma}\tilde{c}_{\alpha\sigma}\tilde{c}_{\sigma\eta}\tilde{c}_{\eta\mu}\tilde{c}_{\mu\varepsilon} + \tilde{c}_{\beta\varepsilon}\tilde{c}_{\alpha\sigma}\tilde{c}_{\sigma\eta}\tilde{c}_{\eta\mu}\tilde{c}_{\mu\gamma}) + \cdots.\end{aligned} \tag{A13}$$

This should be analyzed together with the following general form for the free energy:

$$A^*(\tilde{\mathbf{c}}) = A^*(I_1, I_2, I_3), \tag{A14}$$

where $I_2 = \mathrm{tr}(\tilde{\mathbf{c}} \cdot \tilde{\mathbf{c}})$. Differentiating Eq. (A14) with respect to $\tilde{\mathbf{c}}$ gives

$$\frac{\delta A^*}{\delta \tilde{c}_{\alpha\beta}} = \frac{1}{2}[h_1(I_1, I_2, I_3)\delta_{\alpha\beta} + h_2(I_1, I_2, I_3)\tilde{c}_{\alpha\beta} - h_3(I_1, I_2, I_3)\tilde{c}^{-1}_{\alpha\beta}], \tag{A15}$$

where $h_1(I_1, I_2, I_3) = 2\frac{\delta A^*}{\delta I_1}$, $h_2(I_1, I_2, I_3) = 4\frac{\delta A^*}{\delta I_2}$, and $h_1(I_1, I_2, I_3) = -2I_3\frac{\delta A^*}{\delta I_3}$. Multiplication of Eq. (A13) with Eq. (A15) and performing the same mathematical operations as we did with Eq. (A9) lead eventually to

$$\frac{\delta A}{\delta \tilde{c}_{\alpha\beta}} \Lambda_{\alpha\beta\gamma\varepsilon} \frac{\delta A}{\delta \tilde{c}_{\gamma\varepsilon}} = \sum_{i=1}^{3} \frac{1}{\lambda_i}(h_1\lambda_i + h_2\lambda_i^2 - h_3)^2(f_1 + f_2\lambda_i + f_3\lambda_i^2 + f_3\lambda_i^3 + f_4'\lambda_i^4 + f_4''\lambda_i^4 + f_5'\lambda_i^5 + \cdots). \tag{A16}$$

A sufficient condition for inequality (A16) to be satisfied (taking again into account that the λ_i's should be positive) is

$$f_i \geq 0 \quad \text{for all} \quad i. \tag{A17}$$

For a shear flow, then, it is again found from Eq. (A13) that

$$\Lambda_{zzxx} = \Lambda_{zzxy} = \Lambda_{zzyy} = 0, \tag{A18}$$

$$\Lambda_{zzzz} = 4(f_1\tilde{c}_{zz} + f_2\tilde{c}_{zz}^2 + f_3\tilde{c}_{zz}^3 + f_4'\tilde{c}_{zz}^4 + f_4''\tilde{c}_{zz}^4 + f_5'\tilde{c}_{zz}^5 + \cdots),$$

which leads to

$$(f_1\tilde{c}_{zz} + f_2\tilde{c}_{zz}^2 + f_3\tilde{c}_{zz}^3 + f_4'\tilde{c}_{zz}^4 + f_4''\tilde{c}_{zz}^4 + f_5\tilde{c}_{zz}^5 + \cdots)\alpha_{zz} = 0. \tag{A19}$$

Using that all functions f_i are non-negative [Eq. (A17)] and $\tilde{c}_{zz}$ positive by definition, we conclude again that $\alpha_{zz} = 0$. Hence, higher-order expansions in the expression for $\boldsymbol{\Lambda}$ do not result in nonzero values of the zz component of the field tensor $\boldsymbol{\alpha}$ as long as the symmetry structure inherent in Eq. (A11), e.g., $f_3 = f_4 = 0$ in Eq. (14), is maintained.

APPENDIX B: PROOF OF $\alpha_{zz} \neq 0$ FOR THE CASE OF Λ GIVEN BY Eq. (14) WITH $f_3 \neq 0$ AND/OR $f_4 \neq 0$

Here we show that if $f_3 \neq 0$ and/or $f_4 \neq 0$ in the general expression for $\boldsymbol{\Lambda}$, Eq. (14) in the main text, can indeed result in nonzero values for α_{zz}. To this, we see that the first-order term with respect to $\tilde{\mathbf{c}}$ in Eq. (14), $\tilde{c}_{\alpha\beta}\delta_{\gamma\varepsilon} + \tilde{c}_{\gamma\varepsilon}\delta_{\alpha\beta}$, which still satisfies Onsager's symmetry requirements [Eq. (A12)], leads to

$$\hat{\tilde{c}}_{zz} = 0 = \Lambda_{zzxx}\alpha_{xx} + 2\Lambda_{zzxy}\alpha_{xy} + \Lambda_{zzyy}\alpha_{yy} + \Lambda_{zzzz}\alpha_{zz} = (f_1\tilde{c}_{zz} + f_2\tilde{c}_{zz}^2)\alpha_{zz} + f_3(\tilde{c}_{zz} + \tilde{c}_{xx})\alpha_{xx} + f_3(\tilde{c}_{zz} + \tilde{c}_{yy})\alpha_{yy}. \tag{B1}$$

Therefore, α_{zz} may not be zero even with the conditions that $f_1(I_1) \geq 0$ and $f_2(I_1) \geq 0$. The same result is obtained when $\boldsymbol{\Lambda}$ contains the additional $\tilde{c}_{\alpha\beta}\tilde{c}_{\gamma\varepsilon}$ second-order term (which again satisfies Onsager's symmetry). To this, we see that for the case of steady shear, the zz component of $\tilde{\mathbf{c}}$ turns out to be

$$\hat{\tilde{c}}_{zz} = 0 = \Lambda_{zzxx}\alpha_{xx} + 2\Lambda_{zzxy}\alpha_{xy} + \Lambda_{zzyy}\alpha_{yy} + \Lambda_{zzzz}\alpha_{zz} = (f_1\tilde{c}_{zz} + f_2\tilde{c}_{zz}^2)\alpha_{zz} + [f_4(\tilde{c}_{zz} + \tilde{c}_{xx}) + f_4\tilde{c}_{zz}\tilde{c}_{xx}]\alpha_{xx} + f_4\tilde{c}_{zz}\tilde{c}_{xy}\alpha_{xy} + [f_4(\tilde{c}_{zz} + \tilde{c}_{yy}) + f_4\tilde{c}_{zz}\tilde{c}_{yy}]\alpha_{yy}, \tag{B2}$$

implying nonzero values for α_{zz} under the conditions that $f_1(I_1) \geq 0$ and $f_2(I_1) \geq 0$.

Modifications similar to the above but extended to higher-order terms in the conformation tensor can also be included in the expression for $\boldsymbol{\Lambda}$ as was done with the terms proportional to f_1 and f_2 in Eq. (A13). However, a word of caution is in order here: although all these modifications of $\boldsymbol{\Lambda}$ are perfectly allowed based on Onsager's symmetry properties and the second law of thermodynamics, one should critically examine their consequences from a physical point of view before actually employing them in real flow calculations. Future efforts here would be very beneficial since they could help formulate rheological models with increased capacity in terms of their ability to describe more accurately the complicated viscoelastic properties of polymeric materials.

*Author to whom correspondence should be addressed; cbaig@iceht.forth.gr

†Author to whom correspondence should be addressed; vlasis@chemeng.upatras.gr

[1] J. E. Mark and B. Erman, *Rubberlike Elasticity: A Molecular Primer* (Wiley, New York, 1988).

[2] P. J. Flory, *Principles of Polymer Chemistry* (Cornell University Press, Ithaca, New York, 1953).

[3] L. R. G. Treloar, *The Physics of Rubber Elasticity*, 3rd ed. (Clarendon, Oxford, 1975).

[4] G. Astarita and G. Marrucci, *Principles of Non-Newtonian Fluid Mechanics* (McGraw Hill, London, 1974).

[5] J. H. Weiner, *Statistical Mechanics of Elasticity* (Wiley, New York, 1983).

[6] R. I. Tanner, *Engineering Rheology* (Clarendon, Oxford, 1985).

[7] R. B. Bird, R. C. Armstrong, and O. Hassager, *Dynamics of Polymeric Liquids, Fluid Mechanics*, 2nd ed. (Wiley, New York, 1987), Vol. 1.

[8] R. B. Bird, C. F. Curtiss, R. C. Armstrong, and O. Hassager, *Dynamics of Polymeric Liquids, Kinetic Theory*, 2nd ed. (Wiley, New York, 1987), Vol. 2.

[9] R. G. Larson, *Constitutive Equations for Polymer Melts and Solutions* (Butterworth-Heinemann, London, 1988).

[10] A. N. Beris and B. J. Edwards, *Thermodynamics of Flowing Systems With Internal Microstructure* (Oxford University Press, Oxford, 1994).

[11] F. A. Morrison, *Understanding Rheology* (Oxford University Press, New York, 2001).
[12] H. C. Öttinger, *Beyond Equilibrium Thermodynamics* (Wiley-Interscience, Hoboken, New Jersey, 2004).
[13] V. G. Mavrantzas and D. N. Theodorou, Macromolecules **31**, 6310 (1998).
[14] H. Giesekus, J. Non-Newtonian Fluid Mech. **11**, 69 (1982).
[15] N. Phan-Thien and R. I. Tanner, J. Non-Newtonian Fluid Mech. **2**, 353 (1977).
[16] N. Phan-Thien, J. Rheol. **22**, 259 (1978).
[17] A. I. Leonov, Rheol. Acta **15**, 85 (1976).
[18] A. I. Leonov and A. N. Prokunin, Rheol. Acta **19**, 393 (1980).
[19] P. J. Flory, *Statistical Mechanics of Chain Molecules* (Wiley, New York, 1969).
[20] H. R. Warner, Jr., Ind. Eng. Chem. Fundam. **11**, 379 (1972).
[21] J. M. Wiest, Rheol. Acta **28**, 4 (1989).
[22] A. K. Doufas, I. S. Dairanieh, and A. J. McHugh, J. Rheol. **43**, 85 (1999).
[23] A. K. Doufas, J. Rheol. **50**, 749 (2006).
[24] R. J. Gordon and W. R. Schowalter, Trans. Soc. Rheol. **16**, 79 (1972).
[25] M. W. Jonson, Jr. and D. Segalman, J. Non-Newtonian Fluid Mech. **2**, 255 (1977).
[26] J. L. White and A. B. Metzner, J. Appl. Polym. Sci. **7**, 1867 (1963).
[27] A. Souvaliotis and A. N. Beris, J. Rheol. **36**, 241 (1992).
[28] K. D. Housiadas and A. N. Beris, J. Non-Newtonian Fluid Mech. **140**, 41 (2006).
[29] P. S. Stephanou, C. Baig, and V. G. Mavrantzas, J. Rheol. **53**, 309 (2009).
[30] V. G. Mavrantzas and H. C. Öttinger, Macromolecules **35**, 960 (2002).
[31] M. Laso and H. C. Öttinger, J. Non-Newtonian Fluid Mech. **47**, 1 (1993).
[32] H. C. Öttinger, B. H. A. A. van den Brule, and M. A. Hulsen, J. Non-Newtonian Fluid Mech. **70**, 255 (1997).
[33] J. Q. Broughton, F. F. Abraham, N. Bernstein, and E. Kaxiras, Phys. Rev. B **60**, 2391 (1999).
[34] W. E, B. Engquist, and Z. Huang, Phys. Rev. B **67**, 092101 (2003).
[35] W. E and B. Engquist, Commun. Math. Sci. **1**, 87 (2003).
[36] W. E, B. Engquist, X. Li, W. Ren, and E. Vanden-Eijnden, Comm. Comp. Phys. **3**, 367 (2007).
[37] I. G. Kevrekidis, C. W. Gear, J. M. Hyman, P. G. Kevrekidis, O. Runborg, and C. Theodoropoulos, Commun. Math. Sci. **1**, 715 (2003).
[38] S. Namilae, D. M. Nicholson, P. K. V. V. Nukala, C. Y. Gao, Y. N. Osetsky, and D. J. Keffer, Phys. Rev. B **76**, 144111 (2007).
[39] P. Ilg, H. C. Öttinger, and M. Kröger, Phys. Rev. E **79**, 011802 (2009).
[40] H. C. Öttinger, MRS Bull. **32**, 936 (2007).
[41] C. Baig and V. G. Mavrantzas, Phys. Rev. Lett. **99**, 257801 (2007).
[42] D. N. Theodorou, Chem. Eng. Sci. **62**, 5697 (2007).
[43] D. N. Theodorou, Mol. Phys. **102**, 147 (2004).
[44] V. G. Mavrantzas, T. D. Boone, E. Zervopoulou, and D. N. Theodorou, Macromolecules **32**, 5072 (1999).
[45] R. Kubo, M. Toda, and N. Hashitsume, *Statistical Physics, Nonequilibrium Statistical Mechanics*, 2nd ed. (Springer, Berlin, 1991), Vol. II.
[46] H. Grabert, *Projection Operator Techniques in Nonequilibrium Statistical Mechanics* (Springer, Berlin, 1982).
[47] M. Doi and S. F. Edwards, *The Theory of Polymer Dynamics* (Oxford University Press, New York, 1986).
[48] R. Everaers, S. K. Sukumaran, G. S. Grest, C. Svaneborg, A. Sivasubramanian, and K. Kremer, Science **303**, 823 (2004).
[49] M. Kröger, Comput. Phys. Commun. **168**, 209 (2005).
[50] C. Tzoumanekas and D. N. Theodorou, Macromolecules **39**, 4592 (2006).
[51] A. Brandt, *Multiscale and Multiresolution Methods: Theory and Applications*, Lecture Notes in Computational Science and Engineering Vol. 20, edited by T. J. Barth, T. Chan, and R. Haimes (Springer-Verlag, Berlin, 2002), p. 3.
[52] T. Spyriouni, C. Tzoumanekas, D. N. Theodorou, F. Müller-Plathe, and G. Milano, Macromolecules **40**, 3876 (2007).
[53] S. R. de Groot and P. Mazur, *Non-Equilibrium Thermodynamics* (Dover, New York, 1984).
[54] R. C. Tolman, *The Principles of Statistical Mechanics* (Oxford University Press, London, 1938).
[55] L. D. Landau and E. M. Lifshitz, *Statistical Physics*, Course of Theoretical Physics Vol. 5, 3rd ed. (Butterworth-Heinemann, London, 1976), Pt. 1.
[56] H. B. Callen, *Thermodynamics and an Introduction to Thermostatistics*, 2nd ed. (Wiley, New York, 1985).
[57] M. P. Allen and D. J. Tildesley, *Computer Simulation of Liquids* (Clarendon, Oxford, 1987).
[58] D. J. Evans and G. P. Morriss, *Statistical Mechanics of Nonequilibrium Liquids* (Academic, New York, 1990).
[59] B. D. Todd and P. J. Daivis, Phys. Rev. Lett. **81**, 1118 (1998).
[60] M. E. Tuckerman and G. J. Martyna, J. Phys. Chem. B **104**, 159 (2000).
[61] C. Baig, B. J. Edwards, D. J. Keffer, and H. D. Cochran, J. Chem. Phys. **122**, 114103 (2005).
[62] S. Nosé, Mol. Phys. **52**, 255 (1984).
[63] W. G. Hoover, Phys. Rev. A **31**, 1695 (1985).
[64] A. W. Lees and S. F. Edwards, J. Phys. C **5**, 1921 (1972).
[65] A. M. Kraynik and D. A. Reinelt, Int. J. Multiph. Flow **18**, 1045 (1992).
[66] P. V. K. Pant and D. N. Theodorou, Macromolecules **28**, 7224 (1995).
[67] J. I. Siepmann, S. Karaborni, and B. Smit, Nature (London) **365**, 330 (1993).
[68] C. Baig, B. J. Edwards, D. J. Keffer, H. D. Cochran, and V. A. Harmandaris, J. Chem. Phys. **124**, 084902 (2006).
[69] M. Tuckerman, B. J. Berne, and G. J. Martyna, J. Chem. Phys. **97**, 1990 (1992).
[70] N. C. Karayiannis, V. G. Mavrantzas, and D. N. Theodorou, Phys. Rev. Lett. **88**, 105503 (2002).
[71] It can be verified that a simple linear superposition of multiple conformation tensors (i.e., the generalized Maxwell model or the Rouse model) would not resolve the issue as long as a zero value of α_{zz} is chosen for each individual mode. Only by allowing for an empirical coupling between different modes of the conformation tensor, one might lead to nonzero value of α_{zz} in certain cases; this is, however, not recommended since one would generally not be able to justify such a coupling on physical grounds.
[72] C. Baig, B. J. Edwards, and D. J. Keffer, Rheol. Acta **46**, 1171 (2007).

[73] T. Ionescu, B. J. Edwards, D. J. Keffer, and V. G. Mavrantzas, J. Rheol. **52**, 105 (2008).
[74] V. A. Harmandaris, N. P. Adhikari, N. F. A. van der Vegt, and K. Kremer, Macromolecules **39**, 6708 (2006).
[75] M. Müller and F. Schmid, Adv. Polym. Sci. **185**, 1 (2005).
[76] K. C. Daoulas, M. Müller, M. P. Stoykovich, S. M. Park, Y. J. Papakonstantopoulos, J. J. de Pablo, P. F. Nealey, and H. H. Solak, Phys. Rev. Lett. **96**, 036104 (2006).